


CZECH TECHNICAL UNIVERSITY IN PRAGUE

FACULTY OF NUCLEAR SCIENCE AND PHYSICAL ENGINEERING

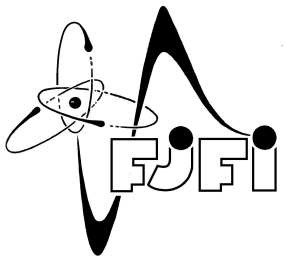

BACHELOR THESIS

STUDY OF B-QUARK PRODUCTION IN DECAY CHANNELS WITH J/ψ ON ATLAS AT LHC

Jaroslav Günther

Supervisor: Václav Vrba, CSc.

July 9, 2007

Foreword

Many of my thanks belong especially to my supervisor Václav Vrba for his inspiring and valuable guidance and providing me a lot of experience with the current physical praxis in the field of really beautiful particle physics. I am very thankful to Maria Smizanska for discussions about the decay chanels with J/ψ (bound state $c\bar{c}$ quarks) which I tried to analyze and to Antonio Pitch for answering my questions concerning the theory of the Standard Model. I appreciate very much the aid of Pavel Řezníček and Christos Anastopoulos who provided me valuable advices and the discussions about object-oriented programming. Particularly I was aided in b-physics reconstruction algorithms and offline analysis by these messieurs. I should thank my colleague Pavel Jež for introducing me to the Athena framework and for useful hints with LaTeX and ROOT. I am also grateful to Guido Negri, Xavier Espinal and Jiří Chudoba for many useful discussions about GRID and for helping me with computing issues related to GRID shifts I participated in. Not least word of thanks go to Institute of Physics in Prague whereby I was allowed to spend several months in the CPPM and CERN laboratories which gives me very much, not only of the b-physics point of view. This thesis mostly rest on the experience and informations I gathered there.

Prohlášení

Prohlašuji, že jsem svou bakalářskou práci vypracoval samostatně a použil jsem pouze podklady uvedené v přiloženém seznamu.

Nemám závažný důvod proti užití tohoto školního díla ve smyslu §60 Zákona č. 121/2000 Sb., o právu autorském, o právech souvisejících s právem autorským a o změně některých zákonů (autorský zákon).

Declaration

I declare that I wrote my bachelor thesis independently and exclusively with the use of cited bibliography.

I agree with the usage of this thesis in the purport of the Act 121/2000 (Copyright Act).

Praha, July 9, 2007 Jaroslav Günther

Název práce:
Studium produkce b-kvarku v rozpadových kanálech s J/psi pomocí ATLAS na LHC

Autor: Jaroslav Günther

Obor: Matematické inženýrství

Druh práce: Bakalářská práce

Vedoucí práce: Václav Vrba, CSc. Katedra fyziky, Fakulta jaderná a fyzikálně inženýrská, České vysoké učení technické v Praze

Abstrakt:

Práce na počátku poskytuje shrnutí fyzikální teorie Standardního Modelu, které se pak dále přes mnoho volných parametrů této teorie odvíjí směrem k otázkám současné částicové fyziky. Teoretický formalismus postupně přechází v potřebu konkrétních experimentálních měření pro ověření popřípadě dalšímu rozvoji fyzikálního pohledu na realitu. Následně jsou popsány některé vzácné rozpady těžkých kvarků, které se svými vlastnostmi vážou k narušení CP symetrie a je provedena autorova analýza jednoho z nich generovaného, simulovaného a rekonstruovaného příslušnými programy v detektoru ATLAS. V další části práce se zabývam popisem čtyř největších stavěných experimentálních zařízení v CERN v LHC urychlovači: ATLASem, CMS detektorem, detektorem ALICE a detektorem LHCb. Dále pak je stručně popsán systém sběru dat z detektoru ATLAS a je načrtnut postup jejich analýzy pomocí současných softwarových nástrojů. V poslední kapitole se práce věnuje distribuci objemných experimentálních dat z experimentu LHC a jejich analýze v rámci celosvětové síte GRID, jakožto jedinému realizovatelnému řešení předpokládaného běhu experimentu.

Klíčová slova: standardní model, ATLAS, analýza, GRID, computing, vzácné rozpady B-mesonů

Title: **Study of B-Quark Production in decay cannels with J/ψ on ATLAS at LHC**

Author: Jaroslav Günther

Abstract:

At the beginning this thesis gives the reader narrow summary of the Standard Model theory. Through the number of free parameters, we come to the questions of today's particle physics. The theoretical formalism is leaved in order to put emphasis on concrete experimental measurements which are needed to confirm or eventually extend the physical view of the reality. In the next chapter are described some of the rare heavy quark decays, which are important to measure the CP symetry. The analysis of one of such decay is done by the author with respect to the ATLAS detector. The third chapter provide the describtion of the CERN accelerator complex and the largest LHC experiments, in particular of ATLAS, CMS, ALICE and LHCb. It shows the main goals and expectations of the physics programme. After that it is devoted to ATLAS Data acquisition system and to the model of the ATLAS analysis. The system with all the software tools is briefly outlined. The last chapter deal with the extensive experimental data distribution and with the analysis of the data within the GRID as the only possible way how to realize the run of such LHC project.

Key words: Standard Model, ATLAS, Analysis, GRID, computing, rare B-decays

Contents

Chapter 1

The Standard Model: Very Short Introduction

"Understanding nature is one of the noblest endeavors the human race has ever undertaken"

Steven Weinberg

1.1 Introduction

Since the beginning of mankind, thinkers have admired the symetry in the nature. Its principles have guided them up to present closer understanding, the Standard Model. The behaviour of a system may be derived with help of the "Noether's theorem". It states, essentially, that for every continuous symetry of Nature there exist a corresponding conservation law,e.g. space homogenity → conservation of momentum, revolving symetry → conservation of angular momentum, time translation → conservation of energy. Since the interactions in microworld are more varied than in 'classical physics' there stands symmetries for the best tool to describe the interactions. Within the limitations of our present technical ability the Standard Model is a computable theory of basic
constituents of physical world :

Fermions - have half-integral spin and systems of identical fermions can be described with a symetric wave function. Leptons and Quarks belong to this class of particles and make up "ordinary matter".

Bosons - are particles with integral spin. Systems of these identical constituents can be described with an antisymetric wave function. All interactions which affect matter particles are due to an exchange of these Force carrier particles.

Spinless Higg's boson/s ? - this part of theoretical predictions of the elektroweak spontaneous symmetry breaking devoid of experimental prove up to the present. Higgs particles are supposed to be givers of mass. So $W^{\pm}$ and Z^0 and all fundamental particles aquire mass by Higgs mechanism (inspired by Goldstone model).

and fundamental interactions :

Electromagnetic interaction - is a long-range (infinity) interaction which affects only particles with non-zero electric charge. Due to its massless force carriers photons γ atoms (and molecules thanks residual force) can exist. These interactions are described in quantum electrodynamic (QED) which is precise tested Quantum field theory application.

Weak interaction - is the interaction responsible for quark or lepton change of type via very massive gauge bosons $W^{\pm}$ and Z^0. By the reason of their large masses (80-100 GeV) is the weak force short range (10^{-17}m). It affects only the particles with non-zero weak-charge. We have six flavours (types) corresponding to each of three generation of matter and antimatter. In 1960's was formulated beautiful unification, electroweak theory by S. L. Glashow, S. Weinberg and A. Salam (GWS).

Strong interaction - is intermediated by massless gluon. As well as the two previous interactions the strong one is a selective interaction which affects only the particles with non-zero color-charge. Strong processes conserve flavour and is flavour-independent. Its range is short (10^{-15}m) probably due to antiscreening of the color field. The theory which describes this interaction is the non-Abelian gauge theory called Quantum Chromodynamics (QCD).

The fourth force is gravity. The gravitational force between the fundamental particles is really weak e.g. between two protons is 10^{36} times weaker than the electrostatic force between them. Indeed, the gravitational interaction in particle physics experiments are utterly negligible.

Physics is really deeply connected with mathematics of symetry, which is provided by the group theory. The Standard Model is a gauge quantum field theory, based on the principles of relativity, quantum mechanics and gauge invariance. The first component of the overall gauge group is $SU(3)_C$ (corresponds to three possible color charges of quarks) and represents QCD. Subscript C express that there are eight gauge bosons = gluons of QCD (one gluon can carry only eight combinations of 3 color + 3 anticolor charge) which couple only to the color charged quarks. The next part of $SU(2)_L \otimes U(1)_Y$ represents the electroweak interaction where the subscripts L and Y indicate that the $SU(2)$ group couples only to the left-handed particles and that the $U(1)$ part couples only to weak-hypercharged particles. From the theory of spontaneous symetry breaking four gauge bosons of $SU(2)_L \otimes U(1)_Y$ the $W^{\pm}$ and Z^0 bosons of the weak interaction and the massless photon of QED arise.

The Standard Model does not provide a complete theoretical framework of physics, since there are important questions which does not answer like e.g. the integration of gravity into the mathematics of the quantum theory of the Standard Model and much more unsolved questions see Section 1.2.4. But thinkers still believe that the nature will not hide herself.

1.2 Theoretical framework

As far as we know the first known steps to describe the world lead us to the Babylonians (15th century BC) who introduced the metric system of flat 2-dimensional space by observation. Even though they mainly effort was to keep track of land for legal and economic purposes and do so for their commercial profit and not for describing the world in terms of science ,like Greeks and many other after them, Babylonian clay cuneiform tablets contain except business transaction records some very old scientific data which still have timeless value. From the beginning of contemporary physics in the 17th century it has been growing up into two parallel directions,

empirical and mathematical. Each of them has its own role. Mathematical methods are used for the description of the hypothetical physical ideas and making mathematical interferences from these hypothesis. Such mathematical interferences can be tested empirically by mechanical generation of scientific data with use remote sensors or experimental devices such as accelerators. These tests may or may not validate the theory and this is the theorist's motivation. In the next paragraph I will try to draw up some of the really basic cogitations and results of a logical structure as a framework of a physical theory we need.

1.2.1 Towards Quantum Electrodynamic

By the end of 19th century emerged serious inconsistecies in well known Newtonian mechanics and classical electromagnetism. In 1923 under the guidance of Langevin, who had consulted Einstein, de Broglie presented his doctoral dissertation on "The connection between waves and particles" . He said that if the light had particle properties why the electron could not have them, too ? To understand the laws of motion of small particles must be taken into account their wave nature. De Broglie postulated his ad-hoc quantization law as validity of equations: $E = hf$ and $p = h/\lambda$ for material particles. The above mentioned inconsistencies were solved later by discoveries of special and general relativity (A.Einstein) and quantum mechanics (N. Bohr, M. Born, A. Einstein, W. Heisenberg, M. Planck, W. Pauli, J. von Neumann, E. Schrödinger, P. Dirac, and many others). There is no proof for quantum theory but it is a very succesful theory which is still not in contradiction to nature.

Let us assume a complex separable Hilbert space $\mathscr{H}\{|\Psi\rangle, ...\}$ of square integrable functions **= ket vectors** $L^2(M, \mu)$ on a manifold (space) M. The set of linear functions $\alpha : \mathscr{H} \to \mathbb{C}$ will call set of **bra vectors** (=dual space $\mathscr{H}^* = \{\langle\Phi|, ...\}$).[1] If we consider the classical dynamical system described with Hamiltonian formalism it is possible to derive corresponding quantum system following rules:

Axioms of canonical quantization

❶ The system is requiered to be described by a **state vector** $|\Psi\rangle \in \mathscr{H}$. Both states $|\Psi\rangle$ and $z|\Psi\rangle$, $(z \in \mathbb{C}, z \neq 0)$ describe the same state.

❷ For each physical quantity A (i.e. function on phase space) there is a corresponding Hermitian operator $\hat{A}$ acting on $\mathscr{H}$. Thus, real eigenvalues of an observable $\hat{A}$ represent values which are possible to receive by measuring A.

❸ Moreover, here exist an operator for any physical state $|\Psi\rangle \in \mathscr{H}$ for which this $|\Psi\rangle$ is one of the eigenstates. Thanks to linearity of built theory the principle of superposition is valid. For operators stands the principle of correspondention. They are constructed the same way as the functions in classical mechanics.

$$\hat{A}|n\rangle = a_n|n\rangle \tag{1.1}$$

[1] I am not fully mathematicaly rigorous. I am trying to sketch the theory.

❹ The time development of an observable A in classical mechanic is expressed in terms of the Poisson bracket:

$$\frac{\mathrm{d}A(q,p)}{\mathrm{d}t} = \{A(q,p), H\} \tag{1.2}$$

whereas in a quantum system this is for explicitly time-independent $\hat{A}$ by analogy **Heisenberg's equation of motion:**

$$\frac{\mathrm{d}\hat{A}}{\mathrm{d}t} = \frac{1}{i}[\hat{A}, \hat{H}] \tag{1.3}$$

where $[\hat{A}, \hat{H}] = \hat{A}\hat{H} - \hat{H}\hat{A}$ is the **commutator** of opperators $\hat{A}$ and $\hat{H}$.[2] The fundamental commutation relations for operator of position $\hat{Q}$ and momentum $\hat{P}$ are:

$$[\hat{Q}_i, \hat{Q}_j] = [\hat{P}_i, \hat{P}_j] = 0 \qquad [\hat{Q}_i, \hat{P}_j] = i\delta_{ij} \tag{1.4}$$

We can say that two dynamical variable are **kompatible** if the measurement of the first one does not affect the second, this is fulfiled iff: $[\hat{A}, \hat{B}] = 0$

❺ Let us suppose many systems prepared in the same arbitary state $|\Psi\rangle \in \mathscr{H}$. Then the mean value of the obtained results by measuring each system at time t is equal to:

$$\langle A_t \rangle = \frac{\langle\psi|\,\hat{A}\,|\psi\rangle}{\langle\psi|\psi\rangle} \tag{1.5}$$

Relativistic quantum theory

Now I would like to point out one conserved quantity which is not well discribed by classical quantum mechanics, i.e. **spin**. Let us look at the Lorentz group, strictly speaking at the transformation matrix of inercial systems $S \to S'$ where S' move with respect to S along the x axis [3]:

$$\Lambda_x = \begin{pmatrix} \gamma & -\gamma\beta & 0 & 0 \\ -\gamma\beta & \gamma & 0 & 0 \\ 0 & 0 & 1 & 0 \\ 0 & 0 & 0 & 1 \end{pmatrix} \overset{introduce\ rapidity\ \phi = arctanh(v/c)}{\longrightarrow} \begin{pmatrix} cosh\ \phi & -sinh\ \phi & 0 & 0 \\ -sinh\ \phi & cosh\ \phi & 0 & 0 \\ 0 & 0 & 1 & 0 \\ 0 & 0 & 0 & 1 \end{pmatrix}$$

det $\Lambda_x = 1$ and the analogy with rotation is also evident. According to Noether's theorem, Lorentz symetry collocate with the conservation of spin which also is part of the Lorentz group. For example there is spin invariant under rotation in plane space of time and x axis in similar way like the angular momentum in classical mechanics. Because the particles which we want to describe travel at speeds at or near c is essential to quantum mechanics obey the principles of special relativity.This synthesis as we will see predicts wholly new physical consequences, antimatter.

In quantum mechanics is done change momentum and energy from their variables to their operators. First is taken an non relativistic relation for energy for a free particle[4]. If we combine it with the operators we receive Schödinger equation

$$\vec{p} = -i\vec{\nabla}\ ,\ \vec{E} = i\frac{\partial}{\partial t} \ \to\ \vec{E} = \frac{\vec{p}^2}{2m} \qquad \to \qquad \textbf{Schrödinger equation: } i\frac{\partial}{\partial t}\psi = \frac{\vec{\nabla}^2}{2m}\psi$$

[2] Units in which $\hbar = 1$ and $c = 1$ are used unless otherwise stated explicitly

[3] $\beta = \frac{v}{c}, \gamma = 1/\sqrt{1-\beta^2}$

[4] free particle is supposed unless otherwise stated explicitly

Similar is possible come to relativistic equation. We write these equations using of covariant notation where the space and time go together and we can obtain Klein-Gordon equation:

$$p^\mu = i\partial^\mu = ig^{\mu\nu}\frac{\partial}{\partial x^\nu} \ , \ E = \vec{p}^2 + m^2 \ \rightarrow \quad \textbf{Klein-Gordon equation: } (\Box + m^2)\phi = 0$$
$$\text{where } \Box = \partial^\mu \partial_\nu$$

This equation describe free particle in a spacetime but to solve it (plane waves for example) we must deal with loose linearity. In 1940‘s Dirac put the question whether it was possible to have linear equation with respect to time which is relativistic, so he had to do something like the square root of the d'Alembertian as follows:

$$-(i\gamma^\nu\partial_\nu + m)[(i\gamma^\mu\partial_\mu - m)]\psi = 0 = (\Box + m^2)\phi \ \rightarrow \quad \textbf{Dirac equation: } (i\gamma^\mu\partial_\mu - m)\psi = 0$$
$$\text{where in order to solve the first equation we have this condition}$$
$$\{\gamma^\mu, \gamma^\nu\} = g^{\mu\nu}, \gamma^0 = \left(\begin{smallmatrix} I & 0 \\ 0 & -I \end{smallmatrix}\right); \vec{\gamma} = \left(\begin{smallmatrix} \vec{\sigma} & 0 \\ 0 & \vec{\sigma} \end{smallmatrix}\right) \text{ and } \vec{\sigma} \text{ are Pauli matrices.} \tag{1.6}$$

γ^μ are four dimensional matrices carrying information about spin of a particle, and the properties of these matrices correspond to properties of the spin $\frac{1}{2}$. Thus, the object which solve the Dirac equation is a four-dimensional and could be divided into two two-dimensional called **spinors** describing matter and antimatter at the same time $\psi = \left(\begin{smallmatrix} \alpha \\ \beta \end{smallmatrix}\right)$. For every plane wave solution of Klein-Gordon equation of the form:

$$\psi(\mathbf{x}, t) = exp[i(\mathbf{px} - Et)] \tag{1.7}$$

there is as well solution ψ^* with negative energy(corresponding momentum -p). If one look at another possible interpretation of Dirac equation:

$$i\frac{\partial\psi}{\partial t} = H\psi$$

and put there the solution it can be seen that the alluded 4 solutions is possible to split in 2 with positive energy corresponding to the two possible spin states of a spin -1/2 particle and two corresponding negative energy solutions. Dirac postulated that the "sea of negative energy states" is fully filled by pairs of electrons in each energy level (spin "up" and "down")And the positive energy states are all unoccupied.Removing negative energy electron from this picture of vacuum produce a hole = positron. Using the ideas of causality in relativity below mentioned quantum field theory explained the development of Dirac equation and the hole theory.

Second Quantization, towards QFT

Due to impossibility mathematicaly describe an exitation and energy release, i.e. when an atom is dropped from one quantum state into another, was quantum field theory developed. This work was done Wendell Furry and Robert Oppenheimer using mathematical framework developed by Vladimir Fock. Let us assume $\mathscr{H}$ (see Section 1.1.) is a Hilbert space of one-particle states and the tensor product also is the space of n particles $\mathscr{H}^{(n)} = \mathscr{H} \otimes \cdots \otimes \mathscr{H}$ where $\mathscr{H}^{(0)} = \mathbb{C}$ is a

ground state (vacuum = state with the lowest energy). Fock established so called Fock space(cf. [1])of an arbitrary number of particles.$\mathscr{F}(\mathscr{H})$ as a direct sum

$$\mathscr{F}(\mathscr{H}) = \sum_{n=0}^{\infty}{}^{\oplus} \mathscr{H}^{(n)}$$

Imagine we have N identical particles which engage states of some dynamic variable.The value a_i is occupied by the number N_i particles(occupation numbers). The state of N identical particles is denoted by:

$$|\phi\rangle \equiv |N_1, N_2, \dots, N_m, \dots\rangle \tag{1.8}$$

Further it is necessary distinguish the description for bosons and fermions.

Bosons

The wave function for bosons is symetrical:$|\psi_1, \psi_2\rangle = |\psi_2, \psi_1\rangle$.Field operators that create or destroy a particle at a particular point in space Let us introduce creation operator $\hat{a}_i^\dagger$ and annihilation operator $\hat{a}_i$ smilar as in the case of harmonic oscilator and new operator $\hat{N}_i$ by:

$$\hat{a_i}^\dagger|\dots, N_{i-1}, N_i, N_{i+1}, \dots\rangle = \sqrt{N_i + 1}|\dots, N_{i-1}, N_i + 1, N_{i+1}, \dots\rangle \tag{1.9}$$

$$\hat{a_i}|\dots, N_{i-1}, N_i, N_{i+1}, \dots\rangle = \sqrt{N_i}|\dots, N_{i-1}, N_i - 1, N_{i+1}, \dots\rangle \tag{1.10}$$

$$\hat{N}_i = \hat{a_i}^\dagger \hat{a_i}$$

$\hat{N}_i$ is operator of number of particles in state i. If these operators act on the 1.8 it is possible to derive folowing commutating relations:

$$[\hat{a_i}, \hat{a_j}] = 0, [\hat{a_i}^\dagger, \hat{a_j}^\dagger] = 0, [\hat{a_i}, \hat{a_j}^\dagger] = \delta_{ij} \tag{1.11}$$

and the operator of the total number of particles then is:

$$\hat{N} = \sum_i \hat{a_i}^\dagger \hat{a_i} \tag{1.12}$$

If total set of observables is continuous then the whole procedure could be repeated for continuous variables for example we can introduce the creation operator into the position x: $\hat{\psi}^\dagger(x)$ and annihilation operator from the position x: $\hat{\psi}(x)$. Commutating relations of these operators are very similar only δ is replaced by dirac delta function $\delta(x-y)$. Now is possible to inroduce the operator of particle number density: $\hat{\mathscr{N}}(x) = \hat{\psi}^\dagger(x)\hat{\psi}(x)$ and the operator of the total number of particles in (a, b) is:

$$\hat{\mathscr{N}}(a, b) = \int_{-\infty}^{\infty} \hat{\psi}^\dagger(x)\hat{\psi}(x) \tag{1.13}$$

This process could be done in more dimensions analogous to the previous. In 1927 Jordan tried to extend the canonical quantization of fields to the wave function which appeared in the quantum mechanics of particles, giving rise to the equivalent name second quantization

for this procedure. When we verge on the system with more undistinguishable particles wave functions are replaced by creation and annihilation operators describing classical continuous fields and the probability of the phenomena $w(x) = \psi^*\psi$ is replaced by operator of particle density $\hat{\mathscr{N}}(x) = \hat{\psi}^\dagger(x)\hat{\psi}(x)$. The latter corresponds to that by the system with more identical particles we express the probability of some phenomena by the operator of particle number density, as well as by real systems.By one particle we can speak about position probability density $\psi^*\psi$.

Fermions

Since fermions can not share quantum states ($|\psi_1, \psi_2\rangle = |\psi_2, \psi_1\rangle \Rightarrow$ satisfy the Pauti exclusion principle) the occupation numbers N_i can only take on the value 0 or 1. Thus, procedure for fermions is the same but it is necessary to take into account the antisymetry of a wave function and all commutating relations must be replaced by the anticommutating ones. Then the operators satisfy $\hat{b}_i^\dagger, \hat{b}_j^\dagger + \hat{b}_j^\dagger, \hat{b}_i^\dagger = 0$ Thus anticommutating relations are: $\{\hat{b}_i, \hat{b}_j\} = 0, \{\hat{b}_i^\dagger, \hat{b}_j^\dagger\} = 0, \{\hat{b}_i, \hat{b}_j^\dagger\} = \delta_{ij}$. And the definitions of continuous operators are the same.

Key position in particle interpretation have Fourier expansions of the solution of equation for classical field (e.g. Klein-Gordon equation for real scalar field). If we find solution which satisfy moreover this commutating relation:

$$\left[\hat{\psi}(t, \mathbf{x}), \hat{\pi}(t, \mathbf{y})\right] = i\delta(\mathbf{x} - \mathbf{y}) \tag{1.14}$$

one could be able to build the annihilation and creation operator(from Fourier expansion of such solution). From the generalized operator of position and generalized momentum other operators can be constructed using the same way as they are built-up in the classical physics. For example bosonic field annihilation operator for a single particle state then may looks like this: $\psi(\mathbf{r}) := \sum_j e^{i\mathbf{k}_j \cdot \mathbf{r}} a_j$ There sould be emphasized that the single particle wave-function is just a scalar field whereas field operator act on the Fock space. Nevertheless, for computing experimentaly useful results from QFT Lagrangians the perturbation theory and Feynman path integrals are really crucial.

Note about Lagrangian formalism

In order to describe symetries the Lagrangian formalism is very effective tool since is obvious from the equatians of motion in classical mechanics that the symetries are not showed in very appropriate way. With this framework the Noether's symetries can be seen immediately there. Since we have relativistic covariance the action is:

$$S = \int_{V^*} d^4x \mathcal{L}(\varphi, \partial_\mu \varphi) \tag{1.15}$$

where is supposed coordinates-explicitly independent lagrangian density which depend on fields and which one integrates over all space-time V^*. Now by using Hamiltonian principle the variation of an action is made to get Lagrangian equation of motion, $\delta S = 0 \rightarrow$

$$\frac{\delta \mathcal{S}}{\delta \varphi} = \frac{\partial \mathcal{L}}{\partial \varphi} - \partial^\mu \left(\frac{\partial \mathcal{L}}{\partial(\partial^\mu \varphi)} \right) = 0 \tag{1.16}$$

But how the lagrangian density look like? That what discribe our dynamical system are Klein-Gordon and Dirac equation. Thus the corresponding lagrangian densities are:

$$\mathcal{L}_{\mathcal{KG}} = \partial^\mu \varphi^* \partial_\mu \varphi - m^2 \varphi^* \varphi \qquad \Rightarrow \qquad (\Box + m^2)\varphi = 0 \ ^5 \tag{1.17}$$

$$\mathcal{L}_{\mathcal{D}} = \overline{\varphi}(i\gamma^\mu \partial_\mu - m)\varphi \qquad \Rightarrow \qquad (i\gamma^\mu \partial_\mu - m)\varphi = 0 \tag{1.18}$$

$$\text{where } \overline{\varphi} \equiv \varphi^\dagger \gamma^0$$

Quantum Electrodynamics and gauge symetry

Eletromagnetism is essentially a theory of light i.e. photons are phenomena which propagate to the speed of light also it is a relativistic system.Thus, if we use the appropriate language where space and time are the same then all electromagnetic phenomenona can be described by Maxwell equations which can be written in covariant notaton:

$$\partial_\mu F^{\mu\nu} = \Box A^\nu - \partial^\nu (\partial_\mu A^\mu) = J^\nu \tag{1.19}$$

where tensor $F^{\mu\nu}$ is a four dimensional curl, $F^{\mu\nu} = \partial^\mu A^\nu - \partial^\nu A^\mu$, $A = (V, \vec{A})$ is a potential and $J^\nu = (\rho, \vec{J})$ is a four-current. Gauge invariance is tha fact that one have infinytely many potentials $A^\mu = A^\mu + \partial^\mu \Lambda^\mu$ which gives the same physics (the same $F^{\mu\nu}$, Λ is arbitrary scalar function). Since, two derivatives of F commute while F is an antisymetric tensor $\Rightarrow \partial^\nu \partial_\mu F^{\mu\nu} = 0$ is here 1.19 written fundamental property of electromagnetism that the current is conserved. Let us do a choice of potential first which satisfy so-called Lorentz gauge $\partial_\mu A^\mu = 0$ and we assume a free particle $J^\mu = 0$ then we obtain the Klein Gordon equation for a massless particle - photon : $\Box A^\mu = 0$. We made one constraint on A^μ,but since A^μ have 4 component it is possible to make 3 residual constraint without changing the electromagnetic field, one such could be: $\Box \Lambda = 0$ and we still have 2 degrees of freedom which corresponds to only two photon polarizations.

One can look at the symetries of lagrangian density for isolated free electron 1.18. If the phase of the field φ is changed $\varphi' = \mathrm{e}^{iQ\theta}\varphi$ then lagrangian with φ' and $\overline{\varphi}' = \mathrm{e}^{-iQ\theta}$ is not. Absolut phases are not observables. Therefore two observers stationed in two diferent points in spacetime should be free to chose the phase in an completely independent way and this principle is called Gauge principle: Two phases should hold locally $\theta = \theta(x)$. Obviously locally this is not the truth $\Leftarrow \partial_\mu \varphi = \mathrm{e}^{iQ\theta}(\partial_\mu + iQ\partial\theta)\varphi$! What about adapt the lagrangian to agree with our symetry principle ? It may be so if we replace our derivative with covariant derivative: $D_\mu \varphi = (\partial_\mu - ieQ\mathscr{A}_\mu)\varphi$. We need to investigate how ought to transform the object $\mathscr{A}_\mu$ while $D_\mu \varphi \rightarrow \mathrm{e}^{iQ\theta} D_\mu \varphi$ should transform this way by redefinition the field. There is requisite to operate with an spin-1 field with this transformation properties: $\mathscr{A}_\mu \rightarrow \mathscr{A}_\mu + \frac{1}{e}\partial_\mu \theta$. Constant e is apparently some symetry not fixed property associated with $\mathscr{A}_\mu$ as well as Q is a property of a fermion field. Lagrangian density after substitution is the lagrangian of QED:

$$\mathcal{L}_{QED} = \overline{\varphi}(i\gamma^\mu \partial_\mu - m)\varphi + eQ\mathscr{A}_\mu(\overline{\varphi}\gamma^\mu \varphi) \tag{1.20}$$

[5] Klein-Gordon equation is for a particle with spin=0.

It consist of free lagrangian + interaction term. The intraction term includes an electron current $(\overline{\varphi}\gamma^{\mu}\varphi)$ with associated external field $\mathscr{A}_{\mu}$. This field propagates using the quantum field theory law also to make this field a quantum field is essential to introduce a free lagrangian of it. Only one such exist using gauge invariant $F^{\mu\nu}$:

$$\mathcal{L}_{kinetic} = -\frac{1}{4}F_{\mu\nu}F^{\mu\nu} \tag{1.21}$$

now when we compute the equation of motion we have Maxwell equation:

$$\partial_{\mu}F^{\mu\nu} = -eQ(\overline{\varphi}\gamma^{\mu}\varphi)$$

EM current which is moving throught the space time and which is generatin the EM field has now an explicit expression. Can there be added a mass term to the $\mathcal{L}_{QED}$ like this one? :

$$\mathcal{L}_{mass} = -\tfrac{1}{2}{m_{\gamma}}^{2}A^{\mu}A_{\mu}$$

Now could be recognizable that both the fermion and photon are quantum fields, e is coupling constant and Q an electric charge. The answer on the question above is it can not and there we have the from the symetry following prediction that the photon is a massless particle.

1.2.2 Towards Electroweak unification

In the time the theory which incorporated both electromagnetic and weak interaction emerged then even thought this theory was these days without decisive experimental prove Steven Weinberg, Abdus Salam and Sheldon Glashow shared in 1979 the Nobel prize for *electroweak theory*.A few years later in 1982 the first signs of the $W^{\pm}$ and Z^{0} were seen at CERN. Weak interaction is much more complicated, but we try to derive the lagrangian of these electroweak interaction from the gauge symetry as well. From field theory follow concept of chirality. When we discover a spin there appear matrixes γ^{μ} 1.6. When we construct:

$$P_R := \frac{1+\gamma_p}{2}, \qquad P_L := \frac{1-\gamma_p}{2} \tag{1.22}$$

while $\gamma_p = \gamma^0\gamma^1\gamma^2\gamma^3, P_R^2 = P_R,$ and $P_L^2 = P_L;\ P_RP_L = 0 = P_LP_R$ then it is obvious that it is going on projectors. Thus, we can take any fermion field and separate it into two different components left and right component of the field. If we discovered the properties of the spin we would receive immediately that this degrees of freedom called chiralities correspond with the projection of the angular momentum to the direction of motion degree of freedom in the limit where the particles does not have any mass - absolute chirality (e.g. for particles with spin -1/2 then the helicity can be positive or negative and also denote right handed or left handed particle, easier told by: If the direction of spin is the same as the direction of its motion then the particle is right handed). For mass particles the chirality is called relative since and depend on the observer's reference frame. Separated fields have separated free lagrangians:

$$\mathcal{L} = \overline{\psi}(i\gamma^{\mu}\partial_{\mu} - m)\psi = \overline{\psi_L}i\gamma^{\mu}\partial_{\mu}\psi_L + \overline{\psi_R}i\gamma^{\mu}\partial_{\mu}\psi_R - m(\overline{\psi_L}\psi_R + \overline{\psi_R}\psi_L) \tag{1.23}$$

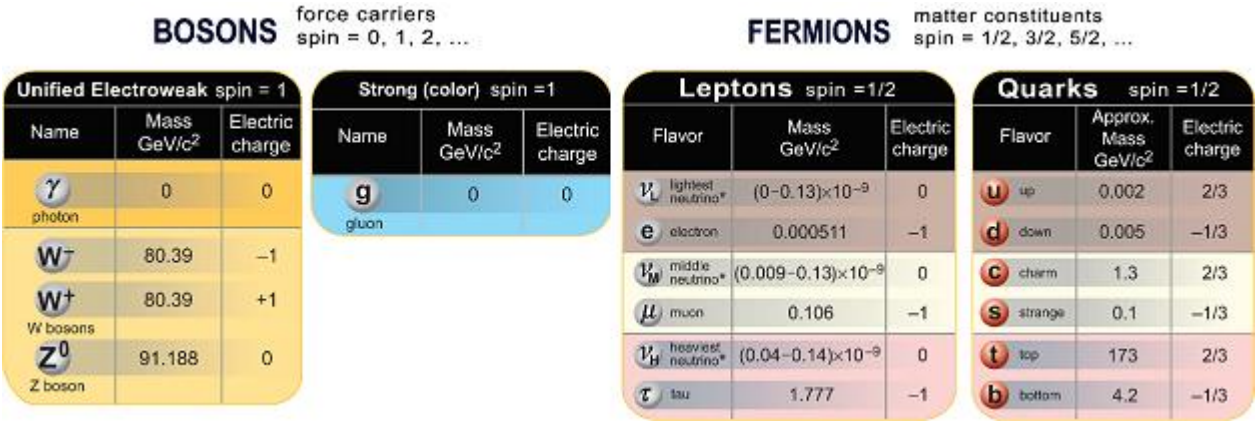

Figure 1.1: Particle chart

Mass is the only one parameter which couples the right and left part, therefore we will deal with the massless particles for this moment using the left projectors.

The theory should satisfy many known experimental facts about particles and their interactions whioch are described further.

Particle Family Structure

Experiment informs us that there are three families of fermions as showed in following particle chart and tell us about its properties.

The three families of particles have the same structure. If we take neutrino and electron than only left-handed part of these fields may couple together into W^-. Right handed components behaves independently. The same is valid for the quarks. Quarks go together to the W^- to make neutron decay for instance, the right parts does not. They participate in other interactions e.g. with photon. Interactions with $W^\pm$ are called charge currents and occurs only by left handed fermions or right handed antifermions. Thanks this interaction flavour may be changed. As well there are flavour conserving neutral current interactions with γ and Z.Moreover, we do not know if right handed neutrino exist. Evidently we need theory which separate left from right.

Electroweak lagrangian

Now we could try to develop electroweak lagrangian using gauge symetry. We take fields for up and down quarks (or for leptons) $\psi_1 \leftarrow \{(q_{up}, q_d)_L \ or \ (l^-, \nu_l)_L\}$; $\psi_2 \leftarrow \{(q_{up})_R \ or \ (\nu_l)_R\}$ and $\psi_3 \leftarrow \{(q_d)_R \ or \ (l^-)_R\}$. We suppose for this moment they are massless for ability to separate right parts from the left ones. The free lagrangian for these fields is:

$$\mathcal{L} = \sum_j i\overline{\psi}_j \gamma^\mu \partial_\mu \psi_j \tag{1.24}$$

Let us suppose for this moment they are massless to have right and left parts separating possible. Obviously there is a $SU(2)_L \otimes U(1)_Y$ symetry. The latter follows similarly to the symetry in QED from the phase changing invariance.The former flavour symetry stands here for additional

(doublet) structure of only one of these fields.If I modify ψ_1 and $\overline{\psi_1}$ by two times two unitary matrix $\mathbf{U_L}$ and by $\overline{\mathbf{U_L}}$ the lagrangian rest unchanged. This matrix just redefines us the "concept of up and down" - changes flavour. Is possible to write:

$$\psi_j \Rightarrow \mathrm{e}^{iy_j\beta}\psi \text{ for } j = 2,\ 3$$
and for $j = 1$ is possible $\psi_1 \Rightarrow \mathrm{e}^{iy_j\beta}\mathbf{U_L}\psi_1$
where $\mathbf{U_L} = \exp\{i\frac{\vec{\sigma}}{2}\vec{\alpha}\}$ and weak isospin change only the left handed component of the field.
(else is analogous to the isospin for strong interaction see Sec.1.2.3)

Let us require this symetry be local $\vec{\alpha}(x) = \alpha,\ \beta(x) = \beta$ and impose to take different conventions for the phases and for the weak isospin labels in different space-time places. Further normal derivative is changed by a covariant derivative which definition is that it transforms exactly the same way as the fields transform. the derivative then we can express like:

$$\mathbf{D}_\mu\psi_1 = [\partial_\mu - ig\mathbf{W}_\mu(x) - ig'y_1B_\mu(x)]\psi_1 \rightarrow \mathrm{e}^{iy_1\beta(x)}\mathbf{U_L}(x)\mathbf{D}_\mu\psi_1$$

$$\mathbf{D}_\mu\psi_{2,3} = [\partial_\mu - ig'y_{2,3}B_\mu(x)]\psi_{2,3} \rightarrow \mathrm{e}^{iy_{2,3}\beta(x)}\mathbf{U_L}(x)\mathbf{D}_\mu\psi_{2,3}$$

where the part which deal with hyper charges y_j is QED like corresponding photon $U(1)$ field B_μ with similar transformation properties: $B_\mu(x) \rightarrow B_\mu(x) + \frac{1}{g'}\partial_\mu\beta(x)$
and from $SU(2)$ symetry the coupling constant g arose together with three new gauge fields (color charge fixed) associated with 2x2 unitary matrices

$$\mathbf{W}_\mu(x) = \frac{\vec{\sigma}}{2}\vec{W}_\mu(x) = \frac{1}{2}\begin{pmatrix} W_\mu^3 & \sqrt{2}W_\mu^\dagger \\ \sqrt{2}W_\mu & -W_\mu^3 \end{pmatrix} \tag{1.25}$$

while $W_\mu = \frac{(W_\mu^1 + iW_\mu^2)}{\sqrt{2}}$
these fields transforms following way: $\mathbf{W}_\mu(\mathbf{x}) \rightarrow \mathbf{U_L}(\mathbf{x})\mathbf{W}_\mu(\mathbf{x})\mathbf{U_L^\dagger}(\mathbf{x})$[6]
$\Rightarrow$ existence of 4 massless gauge bosons.

To derive the lagrangian we substitute the derivative:

$$\sum_j i\overline{\psi}_j\gamma^\mu\mathbf{D}_\mu\psi_j \implies g\overline{\psi}_1\gamma^\mu W_\mu\psi_1 + g'B_\mu\sum_j y_j\overline{\psi}_j\gamma^\mu\psi_j \tag{1.26}$$

Charged current part of the lagrangian corresponds to the up and down quark mixing non-diagonal part of 1.25 and also change flavour:

$$\mathcal{L}_{CC} = \frac{g}{2\sqrt{2}}W_\mu^\dagger\{\overline{q}_{up}\gamma^\mu(1-\gamma_p)q_d + \overline{\nu}_l\gamma^\mu(1-\gamma_p)l\} + Hermitian\ conjugation \tag{1.27}$$

This lagrangian involve the character of muon and neutron decay and lead us to quark-lepton universality (the same coupling constant for both).

[6] $\delta W_\mu^i = \frac{1}{g}\partial_\mu(\delta\alpha^i) - \epsilon^{ijk}\delta\alpha^j W_\mu^k$

Neutral current part collocate with the diagonal of 1.25 and we would like to comprise the interaction with photon and Z:

$$\mathcal{L}_{NC} = gW_{\mu}^{3}\overline{\psi}_{1}\gamma^{\mu}\frac{\sigma_3}{2}\psi_1 + g'B_{\mu}\sum_{j} y_j\overline{\psi}_j\gamma^{\mu}\psi_j \tag{1.28}$$

Even if we would like to predicate that the piece with $B\mu$ correspond to our photon field and the one with W_{μ}^{3} is linked with Z we impact on obstacles with the hypercharges for example in the doublet ψ_1 where then q_{up} and q_d can not have different electric charges. In addition, electromagnetism does not separate left- and right-handed components. We do not now what the part with B_μ or W_{μ}^{3} represent, but suppose the fields are both massless gauge bosons. Let us consider that it is possible to give them a mass by slightly breaking the symetry in order to realize idea that both fields could be quantum superposition of Z and a photon fields in our pieces of lagrangian as follows:

$$\text{orthogonal mixture } \begin{pmatrix} W_{\mu}^{3} \\ B_{\mu} \end{pmatrix} = \begin{pmatrix} cos\ \theta_W & sin\ \theta_W \\ -sin\ \theta_W & cos\ \theta_W \end{pmatrix} \begin{pmatrix} Z_{\mu} \\ A_{\mu} \end{pmatrix} \tag{1.29}$$

Seeing that both fields are neutral in order to A_μ could have the QED interaction following must be satisfied:

$$\text{The same coupling is required: } g\ sin\ \theta_W = g'\ cos\ \theta_W = e \tag{1.30}$$

$$y_1 = Q_\mu - \frac{1}{2} = Q_d + \frac{1}{2} \text{ (halves comes from Pauli matrices), } y_2 = Q_u,\ y_3 = Q_d \tag{1.31}$$

Provided all these relations are precisely satisfied we have fixed the hypercharges $\rightarrow$ photon interaction is defined and provided the interaction in muon decay fixed us θ_W the Z interaction is also fixed. Algebra then reveal us some kind of aproximation to electroweak unificacion where both eletromagnetic and weak interaction come from the same theory:

$$\mathcal{L}_{NC} = eA_\mu \sum_{j} \overline{\psi}_j\gamma^{\mu}Q_j\psi_j + \mathcal{L}_{NC}^{Z} \tag{1.32}$$

$$\mathcal{L}_{NC}^{Z} = \frac{e}{sin\ \theta_W\ cos\ \theta_W} Z_\mu\{\overline{\psi}_1\gamma^{\mu}\frac{\sigma_3}{2}\psi_1 - sin^2\theta_W \sum_{j} \overline{\psi}_j\gamma^{\mu}Q_j\psi_j\} \tag{1.33}$$

where $Q_1 = \left(\begin{smallmatrix} Q_u & 0 \\ 0 & Q_d \end{smallmatrix}\right)$ $Q_2 = Q_u; Q_3 = Q_d$. If the whole procedure is repeated for leptons then the only difference would be electric charges. Interesting question within this framework is if right-handed neutino really exist, because if it do exist then due to zero electric charge which is equal to hypercharge it does not interact neither with photon nor Z and because the W couples only the left handed particles nor with W. This way to our lagrangian also predict that the neutrino does not exist or is there some very weak interaction which allow us to see this object. The last part of the path is to add to the lagrangian the kinetic part for gauge bosons similar to the QED procedure it will be:

$$\mathcal{L}_{kinetic} = -\frac{1}{4}B_{\mu\nu}B^{\mu\nu} - \frac{1}{2}Tr(\mathbf{W}_{\mu\nu}\mathbf{W}^{\mu\nu}) = -\frac{1}{4}B_{\mu\nu}B^{\mu\nu} - \frac{1}{4}(\vec{\mathbf{W}}_{\mu\nu}\vec{\mathbf{W}}^{\mu\nu}) \tag{1.34}$$

$$\text{while } B_{\mu\nu} := \partial_\mu B_\nu - \partial_\nu B_\mu \ \rightarrow\ B_{\mu\nu} \text{ and } \mathbf{W} := \tfrac{i}{g}[\mathbf{D}_\mu, \mathbf{D}_\nu] \ \rightarrow\ \mathbf{U}_L\mathbf{W}_{\mu\nu}\mathbf{U}_L^{\dagger},$$
$$W_{\mu\nu}^{i} = \partial_\mu W_\nu^i - \partial_\nu W_\mu^i + g\epsilon^{ijk}W_\mu^j W_\nu^k$$

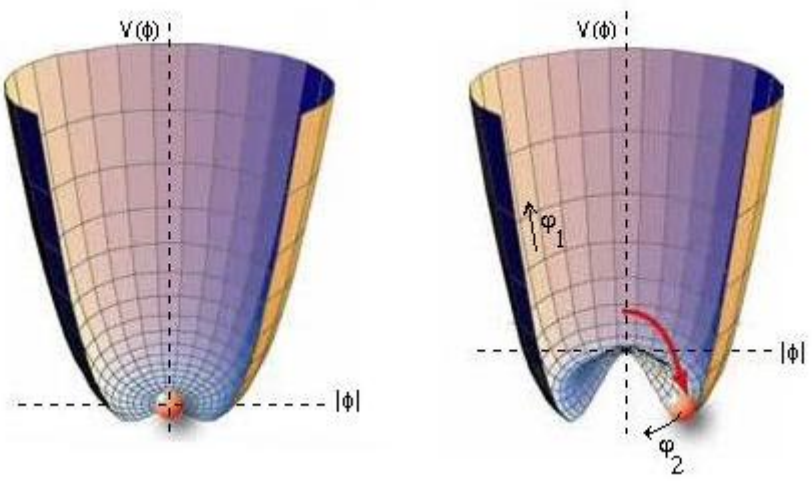

Figure 1.2: Model of Goldstone potential, scalar potencial on the left

The self interaction among the gauge bosons are introduced by the member $g\epsilon^{ijk}W^j_\mu W^k_\nu$ in $W^i_{\mu\nu}$. If we investigated this lagrangian more deeply there appear self-interactions 3 or 4 particles but always both $W\pm$ are presented. However, this lagrangian describe invalid physics. The reason is that this symetry assume all particles massless which e.g. should agree with infinite range of weak interaction and it is not right because of huge mass of W and Z bosons. If we forget about mathematics break our gauge symetry and try to put masses by hand the zero approximation works but any further quantum correction gives infinity, there is a problem of renormalizability and the theory is not predictive. Something should be right.

Spontaneus symetry breaking

There are putted following conditions. We would like to keep symetry in our lagrangian but it is neccesary to do something what will looks like breaking the symetry. Let us imagine birds on the sky who may fly in any direction but suddenly one of them randomly take particular direction and due to very very weak interaction (communication) others follow him. All directions are equivalent also the crucial thing is that they do a choise. In the moment they took one direction then this one is special. And something like that we need in our quantum theory. Suppose potential see Figure 1.2 which has not only one ground state but this state is the generator a continuous symetry then there is an infinite number of ground states and therefore always exist a flat direction (”valey”) which joints different vacuum states which has exactly the same energy. Such potential have a rotational symetry.

To quantize the theory we have to make the choise of our initial particular ground state to make perturbations around that. The quantization is done in non symetric way ..In the moment we do that there is a massless field (particle) which correspond to moving from one ground state to another. The potential depend only on the modulus of ϕ and have following expression:

$$V(\phi) = \mu^2\phi^\dagger\phi + h(\phi^\dagger\phi)^2 \tag{1.35}$$

and corresponding lagrangian:

$$\mathcal{L}(\phi) = \partial_\mu\phi^\dagger\partial^\mu\phi - V(\phi) \tag{1.36}$$

Both potentials in the picture are phase invariant: $\phi(x) \rightarrow e^{i\phi}\phi(x)$. Usually we have the scalar potencial like in the 1.2 where then $h \succ 0,\ \mu^2 \succ 0$. Such potential have trivial single ground vacuum state $\phi = 0 = \phi_0$. Perturbation is represented by movement this particle in state ϕ up and down. It should be noted that ϕ is a function of the space time coordinate x which is supressed to simplify the notation. Let us assume $\mu^2 \prec 0$ then the potential agrees with 'Goldstone potential'. One could try to compute the degenerate minima of this potencial:

$$|\phi_0| = \sqrt{\frac{-\mu^2}{2h}} = \frac{v}{\sqrt{2}},\ V(\phi_0) = -\frac{1}{4}hv^4 = const. \tag{1.37}$$

Let us call v 'vacuum expectation value'. There is a continuus set of possible ground states which correspond to different choises of phase on which the states depends. To quantize the theory we need to make a choise one particular phase = 0. Along the vale the particle have many possible states with the same energy and this movement should corresponds to 0 massless particle and moreover there is direction up the hill. Let us reparametize the field with respect to 2 degrees of freedom the modulus and phase according to the Figure 1.2:

$$\phi := \frac{1}{\sqrt{2}}(v + \varphi_1(x))e^{\frac{i\varphi_2(x)}{v}} \tag{1.38}$$

while at ground state $\varphi_1 = 0$ after that we obtain this lagrangian:

$$\mathcal{L}(\phi) = \frac{1}{2}\partial_\mu\varphi_1\partial^\mu\varphi_1 + \frac{1}{2}(1 + \frac{\varphi_1}{v})^2\partial_\mu\varphi_2\partial^\mu\varphi_2 - V(\phi) \tag{1.39}$$

$$V(\phi) = V(\phi_0) + \frac{1}{2}M^2_{\varphi_1}\varphi_1^2 + hv\varphi_1^3 + \frac{1}{4}h\varphi_1^4 \tag{1.40}$$

$$\Rightarrow\ M^2_{\varphi_1} = -2\mu^2 \succ 0\ ;\ M^2_{\varphi_2} = 0\ \Leftrightarrow\ 1\ massless\ Goldstone\ boson \tag{1.41}$$

Apparently this lagrangian contains two kinetic terms and potential which does not depend on φ_2. This is the essential idea of Goldstone theorem.

Theorem 1 (Goldstone Theorem) *states that whenever a continuous symmetry is spontaneously broken, new massless (or light, if the symmetry was not exact) scalar particles appear in the spectrum of possible excitation. There is one scalar particle - called a Goldstone boson - for each generator of the symmetry that is broken, i.e., that does not preserve the ground state.*

In our case there is an continuus global phase symetry of the potential and kinetic term in our lagrangian is also symetric but only on condition that the phase transformation does not depend on spacetime coordinates otherwise the symetry is broken. In this moment we try to introduce the same phenomena but in the local gauge theory and allow phases to depend on the space time coordinates. In order to give a mass to W and Z SU2 gauge symetry has to be broken. If we take interaction symetry $SU(2)_L \otimes U(1)_Y$ and implement our potential and thus impose new scalar $SU(2)_L$ doublet which differs in electric charge: $\phi(x) = \begin{pmatrix} \phi^{(+)}(x) \\ \phi^{(0)}(x) \end{pmatrix}$ in this theory which is analogous to ψ_1 the field mentioned above ($\mu^2 \prec 0,\ h \succ 0$) we get:

$$\mathcal{L}(\phi) = (\mathbf{D}_\mu\phi)^\dagger\mathbf{D}^\mu\phi - \mu^2\phi^\dagger\phi - h(\phi^\dagger\phi)^2 \tag{1.42}$$

$$\mathbf{D}^\mu\phi = [\partial^\mu - ig\mathbf{W}^\mu - ig'y_\phi B^\mu]\,\phi\ \ ;\ \ \mathbf{W}^\mu = \frac{\vec{\tau}}{2}\vec{W}^\mu \tag{1.43}$$

$$\text{with degenerate vacuum states: } \left|\left\langle 0\left|\phi^{(0)}\right|0\right\rangle\right| = \sqrt{\frac{-\mu^2}{2h}} = \frac{v}{\sqrt{2}} \tag{1.44}$$

Let us look at $\mathbf{D}_\mu\phi$. The $SU(2)$ part and the couplings g and g' should be fixed the same way as in the pervious procedure. In the U(1) sector (with B_μ) we have the only freedom in hypercharge y_ϕ which we fix using the derived relations between hypercharges and electromagnetic charges with regards to **neutral** scalar field $\phi^{(0)}$ which requires the vacuum expectation value and charged $\phi^{(+)} \rightarrow\ y_\phi = Q_\phi - T_3 = \frac{1}{2}$ Thus, if we choose μ^2 negative we have infinite number of ground states which differ by an SU(2) transformation and the doublet field with four degrees of freedom (2 complex fields) could be generally parametrized following way:

$$\phi(x) = \exp\{i\frac{\vec{\tau}}{2}\vec{\theta}(x)\}\frac{1}{\sqrt{2}}\begin{pmatrix}0\\ v+H(x)\end{pmatrix} \text{ in } SU(2) \text{ exponent were added degrees of freedom} \tag{1.45}$$

We have chosen ground state, field with $\vec{\theta} = 0$, as 0 for the charged field and as a vacuum expectation value for the neutral field. The quantum fields which we need for perturbation theory would be excitations over that vacuum. Massive excitation are just a change in moduli. If we the fields $\vec{\tau}$ and $\vec{\theta}$ are set to zero ϕ reprezents the ground state and therefore the lagrangian is exact symetric, but the spontaneous symetry breaking has happened. At this moment we have a local symetry where through the $SU(2)$ transformation may θ rotated away. One is allowed to take a choise of gauge as follows **Unitary gauge:**

$$\vec{\theta}(x) = 0 \implies$$
and kinetic term of our lagrangian takes the form:
$$(\mathbf{D}_\mu\phi)^\dagger\mathbf{D}^\mu\phi \rightarrow \frac{1}{2}\partial_\mu H\partial^\mu H + \frac{g^2}{4}(v+H)^2\{W_\mu^\dagger W^\mu + \frac{1}{2\cos^2\theta_W}Z_\mu Z^\mu\}$$

Manifestly scalar field H is the only one which remains in he game and this term quadratic in the physical W and Z fields. Z field is something what diagonalize the mass term in the lagrangian and currently something what has quadratic field in the lagrangian with a constant v and therefore the Z has got a mass similarly for the W but the photon did not get any mass because the symetry of electromagnetic interaction has not been broken. This theory now could give us predictions for the mass of the gauge bosons:

$$\boxed{M_Z cos\ \theta_W = M_W = \frac{1}{2}vg}$$

To draw up, we started the theory with three gauge bosons which are spin 1 particles and wich are massless, therefore they only have 2 polarizations is means 6 degrees of freedom. With the view of make them massive 3 additional polarizations were needed, so we add by hand these degrees of freedom as goldstone bosons which are spin 0 and are massless. Then our lagrangian is $SU(2)$ symetric and we were able to choose any of a gauge where these goldstones degrees of freedom disappeared and thus was possible to obtain the same physics. These degrees go over to W and Z and so appeared 3 additional polarizations that those particles were missing. That is substance of so called **Higgs mechanism**. Experimentaly is posible to confirm our predictions with muon decay which has very low momentum transfer: From muon lifetime is possible to measure the Fermi coupling constant G_F: $\frac{1}{\tau_\mu} = \frac{G_F^2 m_\mu^5}{192\pi^3}$ and from following equation is obvious the value of our v: $\frac{g^2}{M_W^2 - q^2} \approx \frac{g^2}{M_W^2} := 4\sqrt{2}G_F\ v = (\sqrt{2}G_F)^{-\frac{1}{2}} = 246\ GeV$ Also in conformity with masses of W and Z the weak interaction happens in a scaler of hundred GeV.

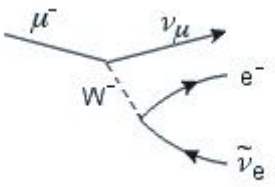

Figure 1.3: Muon decay

However, through the scalar potential ϕ we have introduced four degrees of freedom also the fourth remaining presents massive excitation along the hill of our potential so called **Higgs boson** with a mass which is impossible to predict by reason of one free parameter of the theory = h, $M_H = \sqrt{-2\mu^2} = \sqrt{2h}v$ when we fix it then every couplings are fixed. So lagrangian 1.36 have then this form:

$$\mathcal{L}_S = \frac{hv^4}{4} + \mathcal{L}_H + \mathcal{L}_{HG} \tag{1.46}$$

$$\mathcal{L}_H = \frac{1}{2}\partial_\mu H \partial^\mu H - \frac{1}{2}M_H^2 H^2 - \frac{M_H^2}{2v}H^3 - \frac{M_H^2}{8v^2}H^4 \tag{1.47}$$

$$\mathcal{L}_{HG} = [M_W^2 W_\mu^\dagger W^\mu + \frac{1}{2}M_Z^2 Z_\mu Z^\mu]\{1 + \frac{2}{v}H + \frac{H^2}{v^2}\} \tag{1.48}$$

This piece $\mathcal{L}_{HG}$ show us the possible interactions between Higgs boson and till now experimentaly known gauge bosons. If one would like to write the most general $SU(2) \otimes U(1)$ invariant lagrangian with all degrees of freedom (see Section 1.2.4) and then apply the spontaneous symetry broking there would appear a 'mass' peace of lagrangian from which would be obvious that the masses of fermions are free parametres which are not fixed. But once we know masses then would be all of our couplings fixed and from the lagrangian (interaction piece between fermions and gauge bosons) would be obvious that the higgs boson interact with fermions and the coupling constant is $g_{Higgs} = \frac{m_{fermion}}{v}$.

1.2.3 Footstones of the Quantum Chromodynamics

QCD is similar to QED in that both describe interactions which are mediated by massless spin-1 bosons. The gauge transformation described in QED is a member of $U(1)$ group which is Abelian theory. But very important role in particle physics nowdays play in 1954 by Yang and Mills introduced non-Abelian gauge transformations. Therefore first should be useful to take a glance at $SU(N)$ algebra structure, because for example the QCD is related to $SU(3)$ flavour symetry of quarks.

Basic properties and conventions of algebra $SU(N)$

- Suppose we have $N \times N$ unitary matrices: $UU^\dagger = U^\dagger U = 1$ these matrices could be written as exponentials of $N \times N$ matrices $\mathbf{T}$ (generators) : $U = \exp\ \{i\mathbf{T}^a\theta_a\}; \quad \mathbf{T}^a = \mathbf{T}^{a\dagger}$

- $det\ U = 1$ implies $Tr(\mathbf{T}^a) = 0$

- the number of members of the basis is in general (N^2-1) therefore $a = 1, \ldots, N^2-1$.
- Generally these generating matrices do not commute: $\left[\mathbf{T}^a, \mathbf{T}^b\right] = if^{abc}\mathbf{T}^c$ and
- f^{abc} are called structure constants which fixed us the transformation group if we know whole base of $\mathbf{T}^a$ and are real, antisymmetric.
- Fundamental reprezentation: $\mathbf{T}_F^a = \frac{1}{2}\lambda^a \rightarrow N \times N$

QCD lagrangian

Since last century (the fifties) the first sing of inner structure of nucleons has been known. Experiments in SLAC and DESY $(20GeV)$with scattering electron buches confim this picture in form elastic lepton scattering on point components inside protons called quarks. There are 6 kind of quarks see Figure 1.1 and in relation to strong interaction they can carry three sorts of strong charge called by convention **"color" charge** red, green and blue (and for antimatter antired, antigreen, antiblue). We start with the Dirac lagrangian with this three particle:

$$\mathbf{q} = \begin{pmatrix} q \\ q \\ q \end{pmatrix}$$

$$\mathcal{L} = \overline{\mathbf{q}}[i\gamma^\mu\partial_\mu - m]\mathbf{q}$$

From this notation could be the color $SU(3)$ symetry perceptible. We are allowed to multiply this $\mathbf{q}$ by 3×3 unitary matrix U which 'mix me the collors' and the lagrangian remain unaltered and the new $\mathbf{q}'$ describe me my quark as good as the previous one. First we need to generate unitary transformations in three dimensions this job was done by Gell-Mann who choose these basis:

Commutation relation: $\left[\mathbf{T}^a, \mathbf{T}^b\right] = i\epsilon^{abc}\mathbf{T}^c$

Genetrators of the $SU(3)$ group - Gell-Mann matrices $\mathbf{T}_F^a = \frac{1}{2}\lambda^a$:

$$\lambda^1 = \begin{pmatrix} 0 & 1 & 0 \\ 1 & 0 & 0 \\ 0 & 0 & 0 \end{pmatrix}, \quad \lambda^2 = \begin{pmatrix} 0 & -i & 0 \\ i & 0 & 0 \\ 0 & 0 & 0 \end{pmatrix}, \quad \lambda^3 = \begin{pmatrix} 1 & 0 & 0 \\ 0 & -1 & 0 \\ 0 & 0 & 0 \end{pmatrix},$$
$$\lambda^4 = \begin{pmatrix} 0 & 0 & 1 \\ 0 & 0 & 0 \\ 1 & 0 & 0 \end{pmatrix}, \quad \lambda^5 = \begin{pmatrix} 0 & 0 & -i \\ 0 & 0 & 0 \\ i & 0 & 0 \end{pmatrix}, \quad \lambda^6 = \begin{pmatrix} 0 & 0 & 0 \\ 0 & 0 & 1 \\ 0 & 1 & 0 \end{pmatrix},$$
$$\lambda^7 = \begin{pmatrix} 0 & 0 & 0 \\ 0 & 0 & -i \\ 0 & i & 0 \end{pmatrix}, \quad \lambda^8 = \frac{1}{\sqrt{3}}\begin{pmatrix} 1 & 0 & 0 \\ 0 & 1 & 0 \\ 0 & 0 & -2 \end{pmatrix}$$

where the only non-zero structure constants f^{abc} are

$$\begin{aligned} f^{123} &= 2 \\ f^{147} = -f^{156} = f^{246} = f^{257} = f^{345} = -f^{367} &= 1 \\ f^{458} = f^{678} &= \sqrt{3} \end{aligned} \tag{1.49}$$

Now we impose the same gauge principle which we used to derive QED. Hence, let us assume that two observers placed in two different spacetime points can make their choise of colors in a completely independent way. Let us allow $\theta(x)$ depend on the spacetime coordinate then the the invariance of our lagrangian is spoilt because of the presence of derivative.

$$\mathbf{q} \ \rightarrow \ U\mathbf{g} = \ \exp\{i\frac{\lambda^a}{2}\theta_a\}\mathbf{q}$$

$$\mathbf{D}^\mu\mathbf{q} = (\mathbf{I}\partial^\mu - ig_s\mathbf{G}^\mu)\mathbf{q} \ \rightarrow U\mathbf{D}^\mu\mathbf{q}$$

We add matrix $\mathbf{G}^\mu$ which should cancel the behaviour of derivative. If we impose requirements on $\mathbf{D}^\mu$ transformation it tells us how $\mathbf{G}^\mu$ should transform:

$$\mathbf{D}^\mu \ \rightarrow \ U\mathbf{D}^\mu U^\dagger; \mathbf{G}^\mu \ \rightarrow \ U\mathbf{G}^\mu U^\dagger - \frac{i}{g_s}(\partial^\mu U)U^\dagger$$

$$[\mathbf{G}^\mu]_{\alpha\beta} := \frac{1}{2}(\lambda^a)_{\alpha\beta}G^\mu_a(x)$$

where this $\frac{i}{g_s}(\partial^\mu U)U^\dagger$ cancel the transformation property of the derivative $\mathbf{I}\partial^\mu$ and as one could see the transformation properties are fixed the same way as for the photon field in QED.But in this case is not possible to commute $\mathbf{G}^\mu$ with the transformed one like in QED where it was only a field that is why we need something in addition. Let us expand matrix G in basis of generators λ^a:

$[\mathbf{G}^\mu]_{\alpha\beta} := \frac{1}{2}(\lambda^a)_{\alpha\beta}G^\mu_a(x)$ and we received $\Rightarrow$ 8 Gluon Fields

If we expand the exponential to the first order then appear here infinitesimal transformation like this one:

$\delta q^a = i\delta\theta_a \left(\frac{\lambda^a}{2}\right)_{\alpha\beta} q^\beta$ and so we have the infinitezimal transformation for G^μ_a:

$\delta G^\mu_a = \frac{1}{g_s}\partial^\mu(\delta\theta_a) - f^{abc}\delta\theta_b G^\mu_c$.

The matrices do not commute so $f^{abc} \neq 0$, thus the transformation of the gluon field depends on the gluon field itself, one universal coupling g_s, gauge parameter θ and should be noted that there are no color charges. If we would put q as an arbitrary parameter into the exponencial concurrently with derivation of QED and do some algebra then due to noncommutativity of the matrices at some point the consistency could be broken if the equation $\mathsf{q}^2 = \mathsf{q}$ is not satisfied. This fixes us q :

$$\mathsf{q} = \begin{cases} 0 & \text{for some object without strong interaction (lepton)} \\ 1 & \text{for some object interacting with a gauge field but the color charge is then fixed} \end{cases}$$

In contrast with QED which does not fix me this q (the electric charges are arbitrary) also QCD involves only one single parameter = g_s

Let us look at the 'kinetic' term of QCD lagrangian:

$$\mathbf{G}^{\mu\nu} := \frac{i}{g_s}[\mathbf{D}^\mu, \mathbf{D}^\nu] = \partial^\mu\mathbf{G}^\nu - \partial^\nu\mathbf{G}^\mu - ig_s[\mathbf{G}^\mu, \mathbf{G}^\nu] \rightarrow \ U\mathbf{G}^{\mu\nu}U^\dagger$$

$$G^{\mu\nu} := \frac{\lambda^a}{2}G^{\mu\nu}_a \ \ ; \ \ G^{\mu\nu}_a = \partial^\mu G^\nu_a - \partial^\nu G^\mu_a - g_s F^{abc}G^\mu_b G^\nu_c$$

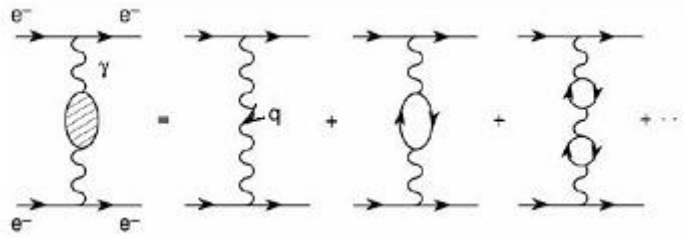

Figure 1.4: Diagrams of quantum corrections in QED

'Kinetic' term of our lagrangian then take the form of 8 kinetic terms for each of 8 gluons:

$$\mathcal{L}_K = -\frac{1}{2}Tr(\mathbf{G}^{\mu\nu}\mathbf{G}_{\mu\nu}) = -\frac{1}{4}G_a^{\mu\nu}G^a_{\mu\nu}$$

But this is not only a kinetic term because if we look at it carefully it contains gluon self-interactions. Three gluon interactions for '$g_s f_{abc}$' and four gluons in the same vertexfor '$g_s f_{abc} f_{ade}$'. Moreover, if we endeavoured to put mass term into the Lagrangian such as: $\mathcal{L}_M = \frac{1}{2}m_G^2 G_a^\mu G_\mu^a$ we would convince that it is not gauge invariant. On this condition we have prediction that $m_G = 0$ gluons are massless. Finall lagrangian of QCD theory then can be written as:

$$\mathcal{L}_{QCD} = -\frac{1}{2}Tr(\mathbf{G}^{\mu\nu}\mathbf{G}_{\mu\nu}) + \overline{\mathbf{q}}[i\gamma^\mu \mathbf{D}_\mu - m_q]\mathbf{q} \tag{1.50}$$

However, this lagrangian fails at low energy states also is not capable of explanation why are quarks confined in the proton ? Now we need to go ahead to quantum theory to explain why the parameter g_s is in our experiments sometimes big and sometimes very small.

Quantum corrections

When we look at interaction of two electrons in classical electrodynamics they exchange a photon. In QED are there several more additional possible processes called quantum corrections. This photon is able to create electron positron pair for a very short amount of time (Heisenberg principle) which then annihilate again. Suppose that it happen more times than it change the field indispensable, see Figure 1.4. All these corrections modify the coupling constant of classical interaction $\alpha \sim e^2$ to effective running coupling :

$$\alpha(Q^2) \approx \frac{\alpha}{1 - \frac{\alpha}{3\pi} log(\frac{Q^2}{m^2})}$$

which depends on Q^2 where Q is a momenta transfer defined as $Q^2 = -q^2$, where q is photon 4-momenta. Significant physical content has the factor of 3 and the negative sign. It tells us that if the momentum transfer is increased than $\alpha(Q^2)$ increases. At higher energies (shorter distances) is the interaction stronger than at lower energies. In vacuum the emited e^+, e^- pairs looks like dipoles ant therefore physical vacuum is not empty and could be interpreted as polarized dielectric medium. If we concern on two opposite charged particles in the vacuum there are many dipoles between them and seen from large distances these all dipoles screening the charge of one of those particles and we observe smaller charge, our interaction is smaller. However, if we increase the energy, we are approching the two charges and as a consequence less dipoles

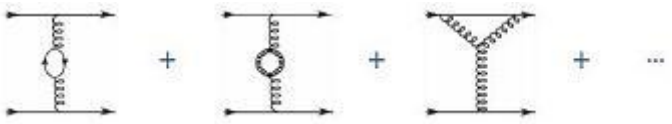

Figure 1.5: Diagrams of quantum corrections in QCD

in the middle are occured. Larger electric charge become evident and the interaction is much larger.

QCD works similar but do the opposite. Gluons have self interactions which dramatically contribute to the quantum correction process, see Figure 1.5. The QCD coupling $\alpha_S = \frac{g_s^2}{4\pi}$ is going to following QCD running coupling formula α_S :

$$\alpha_S(Q^2) \approx \frac{\alpha_S(Q_0^2)}{1 - \beta_1 \frac{\alpha_S(Q_0^2)}{2\pi} log(\frac{Q^2}{Q_0^2})}$$

If coefficient β_1 was calculated it would be negative because the contribution of self-gluon interactions predominate. Whereas quarks screen the color charge gluons have the opposite antiscreening effect. From the formula it is obvious that, the interaction turns weeker at high energies (short distances) on the other hand it comes to very big interaction at large distances (low energies). In addition this feature $\alpha_S(Q^2) \overset{Q^2 \to \infty}{\to} 0$, that the interaction goes to zero at high energies is called asymtotic freedom . At lower energies we go into non-perturbative region where numerical simulations determine that there is some confinement which corresponds with probability of hadronization equal to 1.

1.2.4 CKM matrix and CP violation

The most general $SU(2)_L \otimes U(1)$ invariant lagrangian with "new" scalar doublet ϕ mentioned at the end of Section 1.2.2 could be written following way:

$$\mathcal{L}_Y = (\overline{q}_{up}, \overline{q}_d)_L \left[c^{(d)} \begin{pmatrix} \phi^{(+)} \\ \phi^{(0)} \end{pmatrix} (q_d)_R + c^{(up)} \begin{pmatrix} \phi^{(0)\dagger} \\ -\phi^{(+)\dagger} \end{pmatrix} (q_{up})_R \right] + (\overline{\nu}_l, \overline{l})_L c^{(l)} \begin{pmatrix} \phi^{(+)} \\ \phi^{(0)} \end{pmatrix} l_R$$

$$+ Hermitian\ conjugate$$

The there appeared "three" new couplings c^* which are fully arbitrary. Providing that we consider more indentical copies of the one family structure introduced in Section 1.2.2 and guided by todays experiments generalize up to 3 known generations of matter like : $\begin{pmatrix} \nu'_j & u'_j \\ l'_j & d'_j \end{pmatrix}$ $j = 1, 2, 3$, l_j and ν_j are any lepton ($Q = -1$)and neutrino ($Q = 0$) from one family likewise u_j ($Q = +\frac{2}{3}$) and d_j ($Q = -\frac{1}{3}$)are two flavours of quarks from the same generation. Then the lagrangian takes the form:

$$\mathcal{L}_Y = \sum_{jk} \{ (\overline{u}'_j, \overline{d}'_j)_L \left[c^{(d)}_{jk} \begin{pmatrix} \phi^{(+)} \\ \phi^{(0)} \end{pmatrix} d'_{kR} + c^{(u)}_{jk} \begin{pmatrix} \phi^{(0)\dagger} \\ -\phi^{(+)\dagger} \end{pmatrix} u'_{kR} \right] + (\overline{\nu}'_j, \overline{l}'_j)_L c^{(l)}_{jk} \begin{pmatrix} \phi^{(+)} \\ \phi^{(0)} \end{pmatrix} l'_{kR} \}$$

$$+ Hermitian\ conjugate$$

The fully arbitrary parameters are now matrices c_{jk}. Let us allow the neutral scalar field acquires the vacuum expectation value. Spontaneous symetry breaking uncover us masses of all fermion fields.

$$\mathcal{L}_Y = -\left(1+\frac{H}{v}\right)\{\overline{d}'_L M'_d d'_R + \overline{u}'_L M'_u u'_R + \overline{l}'_L M'_l l'_R + \ Hermitian\ conjugation\} \quad (1.51)$$

$$[M'_d, M'_u, M'_l]_{jk} = -\left[c^{(d)}_{jk}, c^{(u)}_{jk}, c^{(l)}_{jk}\right]\frac{v}{\sqrt{2}} \quad (1.52)$$

Here by d' is understood a vector in flavour states which contains all quarks which are d-like e.g. d,s,b-quarks. All quarks with charge $\frac{-1}{3}$ are also collected in this 3D vector in flavour space. The latter written are arbitrary complex mass matrices. Thus, if weak eigenstates which we put in this family flavour structure 1.2.4 are not generally the same as the eigenstates of mass then there is no reason why those fields should be the normal quarks we are speaking about because the normal quarks we are speaking about are objects with a definite mass. If the mass matrices are diagonalized following way: $M'_d = S^\dagger_d \mathcal{M}_d S_d U_d$ while U and S are unitary matrice and $\mathcal{M}_d$ = $diag(m_u, m_c, mt)$ are mass eigenstates.

$$\mathcal{L}_Y = -\left(1+\frac{H}{v}\right)\{\overline{d}\mathcal{M}_d d + \overline{u}\mathcal{M}_u u + \overline{l}\mathcal{M}_l l + \ Hermitian\ conjugate\} \quad (1.53)$$

Then from the lagrangian is obvious that the mass eigenstates d are really not equal to the weak ones mentioned before d'. The relations between flavour and mass eigenstates are the cause. They could be computed as $d_L = S_d d'_L$ whereas for the right handed field the transformation looks different $d_R = S_d U_d d'_R$. We apriori know only that the mass and weak eigenstates can not be different, but if something is not forbidden by some kind of conservation law it suddenly could happen, also they are really diverse and it looks like it lead us to some mixing among quarks.

Since we would like to work with states with a definite mass we take this transformation relations among the weak and mass eigenstates and implement them into the lagrangian. When we take a field f then $\overline{f}_L f_L = \overline{f}'_L f'_L$ and $\overline{f}_R f_R = \overline{f}'_R f'_R$ and take into account that only the same-handed parts of fields are able to communicate via this interaction then it evokes invariance of the photon and Z couplings (neutral currents see Section 1.28) to this modification $\mathcal{L}_{NC} = \mathcal{L}'_{NC}$. The $W^\pm$ interactions change flavour also they are sensitive to this transformation between two basis and in the lagrangian (in term mass eigenstates) $\mathcal{L}_{CC}$ see Section 1.27 appears supplementary unitary matrix $\mathbf{V_{ij}} = \mathbf{S_u S_d^\dagger}$:

$$\mathcal{L}_{CC} = \frac{g}{2\sqrt{2}} W^\dagger_\mu \left[\sum_{ij} \overline{u}_i \gamma^\mu (1-\gamma_p) V_{ij} d_j + \sum_l \overline{\nu}_l \gamma^\mu (1-\gamma_p) l\right] + Hermitian\ \ conjugation \quad (1.54)$$

Matrix V_{ij} influence the interaction and the only thing we know is that it is unitary. We have got abundance of interesting phenomena - quark mixing. We started with the presumption that the up quark likes couple to the down, charm to the strange, etc. results from the experiment that these are seen ussualy together and we come to the further transitions with smaller probability. We can not predict them because we do not know parameters V_{ij}. If we make the same consideration for leptons than provided right-handed neutrino does not exist and neutrinos have exactly no mass (they are undistinguishable) we came to conclusion that there are no mixing

and separate lepton number conservation holds. Another situation turns up if we presume that ν_R exist and neutrinos have nonzero mass. In this case we get exactly the same phenomena as for quarks and there appears lepton violation in the theory (the separate lepton numbers may not be preserved). But we have many bounds of experiments which tell us that the lepton violation is very suppress.

Let us look at quark mixing matrix in a little bit more detaile. If we had N generations of matter that would mean N^2 arbitrary parametres in our unitary matrix. However no all of them have physical content. Some parameters could be hidden in the field redefinition. By redefinition is meant that if one do this process no parameters go to any observable. We are allowed always to redefine the phase of any field. For example matrix $\mathbf{V_{ij}}$ is coupling up quark to down quark which if are redefined at the same time like the matrix nothing changes:

$$u_i \to \mathrm{e}^{i\phi_i} u_i \; ; \; d_j \to \mathrm{e}^{i\theta_j} d_j$$

$$\Rightarrow \quad \mathbf{V_{ij}} \to \mathrm{e}^{i(\theta_j - \phi_i)} \mathbf{V_{ij}}$$

In case of N generations there is possible to redefine in this way $2N-1$ arbitrary phases. After some careful counting one could investigate that physicaly relevant parameters are $\frac{1}{2}N(N-1)$ = moduli and $\frac{1}{2}(N-1)(N-2)$ complex phases. If there was one generation there would be nothing to mix. In case of two families there is only one parameter - moduli called Cabibbo angle but no complex phase which is essential to violate CP symetry which is therefore exact symetry of this two-family lagrangian. Nowdays we know 3 generations and due to sizeable CP violation e.g. in B^0 decays we know that it is the minimal number of families. There are 3 moduli (angles) and one phase. So-called Cabibbo-Kobayashi-Maskawa (CKM) matrix after parametrization $c_{ij} = cos\ \theta_{ij};\ s_{ij} = sin\ \theta_{ij}$ or so-called Wolfenstein parametrizatiton which uses 4 real parameters $\lambda = s_{12}c_{13} \approx 0.2,\ A,\ \rho,\ \eta$ looks like:

$$\mathbf{V} = \begin{bmatrix} c_{12}c_{13} & s_{12}c_{13} & s_{13}e^{-i\delta_{13}} \\ -s_{12}c_{23} - c_{12}s_{23}s_{13}e^{i\delta_{13}} & c_{12}c_{23} - s_{12}s_{23}s_{13}e^{i\delta_{13}} & s_{23}c_{13} \\ s_{12}s_{23} - c_{12}c_{23}s_{13}e^{i\delta_{13}} & -c_{12}s_{23} - s_{12}c_{23}s_{13}e^{i\delta 13} & c_{23}c_{13} \end{bmatrix}$$

$$\approx \begin{bmatrix} 1 - \frac{\lambda^2}{2} & \lambda & A\lambda^3(\rho - i\eta) \\ -\lambda & 1 - \frac{\lambda^2}{2} & A\lambda^2 \\ A\lambda^3(1 - \rho - i\eta) & -A\lambda^2 & 1 \end{bmatrix} + \mathcal{O}(\lambda^4) \tag{1.55}$$

There should be noted at least some brief information about symetries. Charge conjugation symetry (C) is generated by invariance under particle - antiparticle interchange, parity symetry (P) creates the mirror image of a physical system and T-symetry is symetry under time reversal transformation. In quantum field theory provide **CPT theorem** which states that any Lorentz invariant local quantum field theory with a Hermitian Hamiltonian must preserve causality, charge conugation and parity (have CPT symmetry). This theorem shows that the only way how to violate CP symetry is to violate T-symetry at the same time. Let us consider the time reversal operator and the operator of changing parity as follows: $\mathcal{T}\widehat{X} = \widehat{X}$, $\mathcal{T}\widehat{P} = -\widehat{P}$ and $\mathcal{P}\widehat{X} = -\widehat{X}$, $\mathcal{P}\widehat{P} = -\widehat{P}$, where the $\widehat{X}$ and $\widehat{P}$ are quantum operators for position and momentum. $\mathcal{P}[\widehat{X}, \widehat{P}]\mathcal{P}^{-1} = \frac{i}{2\pi}\hbar$ whereas if the same operation is done for $\mathcal{T}$ then is obvious that $\mathcal{T}i\mathcal{T}^{-1} = -i$ operator of time reversal is an antiunitary operator and also correspond to the complex conjugation. The hamiltonian H of the interaction does depends on V_{ij} then if V_{ij} are complex then $[\mathcal{T}, H] \neq 0$ and therefore is necessary to have complex phase to violate this symetry. Thus,

important is that there is the CP violation only on condition that the phase $\delta \neq 0$ (or $\eta \neq 0$). CP violation has great signifcance because it is the reason why is in the universe matter-dominated.

The large lack of the Standard Model are free parameters: in QCD one α_S then from gauge sector in electro weak theory there are parameters α, G_F and 2 from scalar sector M_Z and M_{Higgs} . From so-called Yukawa sector, couplings between fermions and the Higgs field, there appear 9 masses of fermions, 3 angles θ_i and one phase δ . These 18 arbitrary parameters + neutrino masses and eventually parameters arising from lepton mixing evoked that by far we do not understand everything. We are able only to see experimentaly by measuring these parameters if the processes works how they are supposed to be for example checking the unitarity of CKM matrix. Moreover we have much more questions to solve for instance why we assume only 3 generations, why left-handed parts of fields behave another way then the right one and much more ...

Chapter 2

Rare Heavy Quarks Decays

Rare decays may be classified as these which probability is much smaller than by other possible processes, that means decay with small braching ratio parameter. Hard to say what is really rare, however decays with braching ration $\prec 10^{-3}$ is supposed to be rare. They occur mainly at high energetic colissions what collocate with huge mass of participated particles.

2.1 From theoretical aspects to the experiment

Number of processes prediced by Standard Model has not been observed yet. Heavy quark decays are central to the international effort to test the Standard Model. Powerful probe of the limits of the Standard Model is provided by rare decays, especially the b quark has emerged as the focus of this program. There are many observables and many challenging measurements. They require very large data samples and mastery of strong-interaction effects that obscure our view of the underlying electroweak physics. Since the weak eigenstates of quarks are mixtures of the mass eigenstates stand flavour physics in front of our interest. With three generations, the mixing is described by the Cabibbo-Kobayashi-Maskawa matrix.

$$\mathbf{V} = \begin{bmatrix} V_{ud} & V_{us} & V_{ub} \\ V_{cd} & V_{cs} & V_{cb} \\ V_{td} & V_{ts} & V_{tb} \end{bmatrix} \begin{bmatrix} |d\rangle \\ |s\rangle \\ |b\rangle \end{bmatrix} = \begin{bmatrix} |d'\rangle \\ |s'\rangle \\ |b'\rangle \end{bmatrix}$$

The elements of this matrix describe the probability of transition $|V_{q\bar{q}}|^2$ from one to another quark q. If we do not leave the generation of the mass then the size of this transition probability is larger than in the case of transition probabilities between different generations. The remoter two generations we consider the smaller the probability is. The smallest transition probability is between first and third generation. The unitarity of the CKM matrix assures that the elementary vertices involving neutral gauge bosons (G, Z^0, γ) and the neutral Higgs are flavour conserving. Flavour changing neutral current transitions is also forbidden.

The unitarity of the CKM matrix imposes strong constraints on its elements: $\sum_{ij} V_{ij} V_{ij}^{\dagger} = \delta_{ij}$, where e.g. this $V_{ud}V_{ub}^* + V_{cd}V_{cb}^* + V_{td}V_{tb}^* = 0$ is one of 6 unitary triangles in the complex plane in which is this chapter further engaged. See Figure 2.1. If each member of this equation is divided by the best-known one, $V_{cd}V_{cb}^*$, the most commonly used unitarity triangle arises.

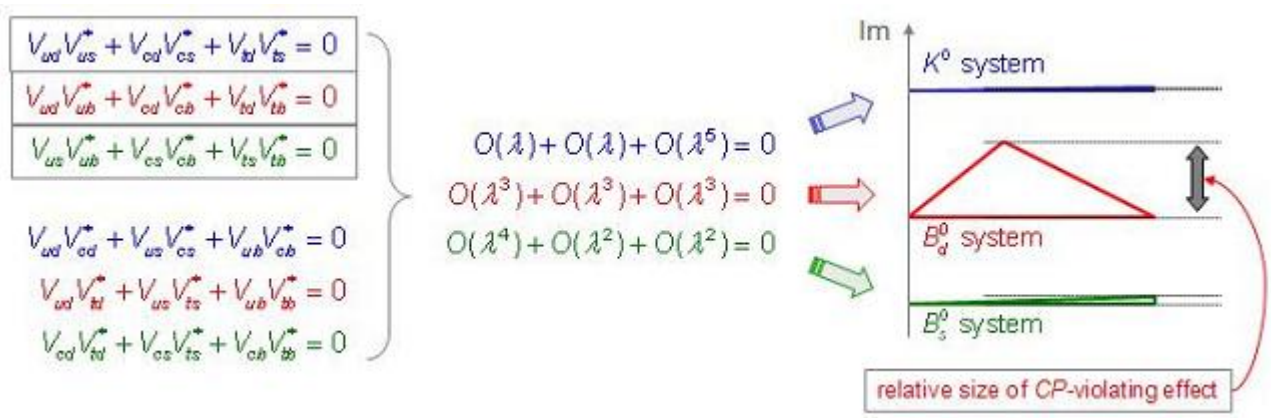

Figure 2.1: Interesting Unitary Triangles which involves different physical processes and indicate the strenght of the CP violation effect as the size of the imaginary axis and the shape of the triangle is proportional to the order of power of λ in the relevant addend of the sum.

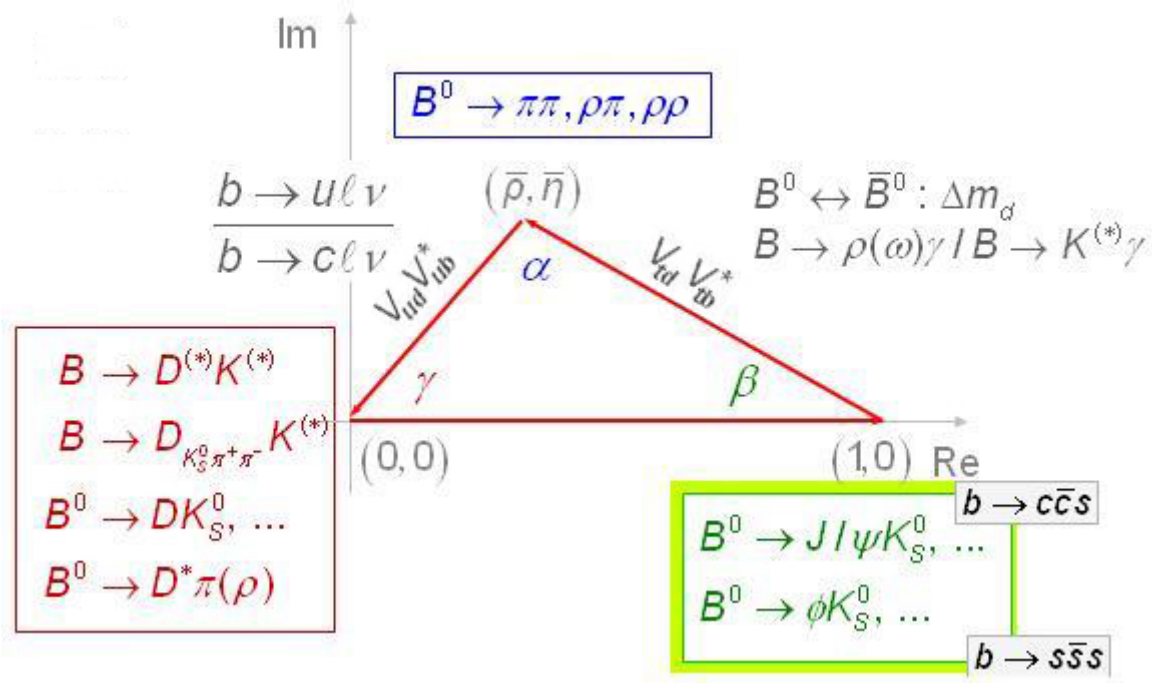

Figure 2.2: Picture of the Unitarity Triangle indicate the examples of B decay modes which give access to its angles and sides.

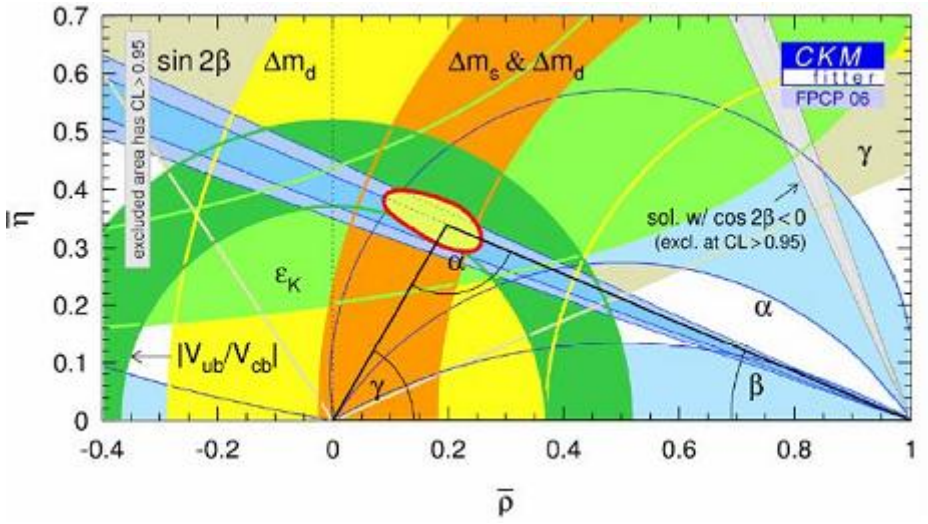

Figure 2.3: Illustration of the current experimental constraints on the CKM Unitarity Triangle.$\overline{\eta} = \eta(1 - \frac{1}{2}\lambda^2),\ \overline{\rho} = \rho(1 - \frac{1}{2}\lambda^2)$.

See the Figure 2.2. Due to the complex conjugate members we are able to test if this matrix is complex or real and also whether the CP is violated or is not. We have there many different ways how to measure these sides of the triangle with many independent observables. Up to now measurements of many decays e.g. $B^0 - \overline{B}^0$ or $B_s - \overline{B}_s$ mixing are all consistent. It was shown following picture of the behaviour of nature, see Figure 2.3. From this point of view is CP violation very rare effect whether thanks to small CP assymetry or due to suppresed decay rates.

It exists three ways how to violate CP symetry: CP violation in mixing of the neutral flavor-antiflavor systems, which is e.g. dominant mechanism for K^0-$\overline{K}^0$ systems, then CP Violation in interference between decays with and without mixing - these are called 'indirect' CP violation and the last possibility is called 'direct' - CP violation in the decay by interference of decay amplitudes with different phases. Effects of mixing of particles with their antiparticles, of particle-antiparticle oscillation, and of CP violation, which are not at all synonymous, were predicted and discovered firstly in the system of the neutral strange mesons $K^0 - \overline{K}^0$, then also quite recently in the neutral B meson systems.

2.2 CP violation and $B_q^0 - \overline{B}_q^0$ mixing , $q = d, s$

Presently there are huge efforts to explore B-meson decays in which is this chapter further engaged. All B-meson decays that do not occur though the usual $b \rightarrow c$ transition are usually called rare. Rare B-meson decays provide an interesting tests of the Standard-Model description of the quark-flavour sector and the CP violation residing there. Thanks to the e^+e^- B factories at KEKB (Belle) and SLAC (BaBaR), CP violation is now a well-established phenomenon in the B-meson system, and recently B_s^0-$\overline{B}_s^0$ mixing could be measured at the Tevatron. The decays of B_s^0 mesons are one of the key targets of the B-physics programme at the LHC (Large Hadron Collider - CERN).Apropos beauty oscillation was first observed as mixing of B_s from

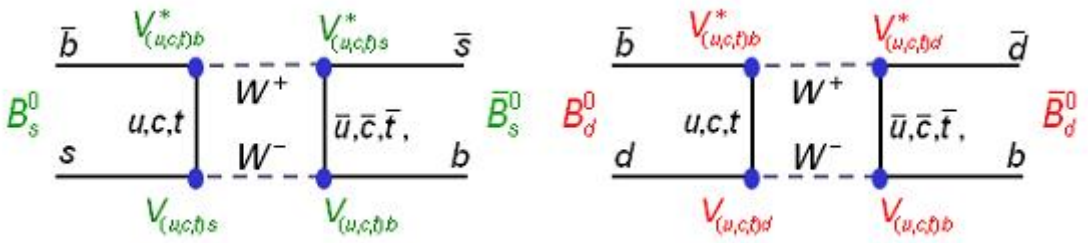

Figure 2.4: Feynman diagrams of $B^0_q - \overline{B}^0_q$ mixing , $q = d, s$

$\Upsilon(4S)$ decays. Due to the big mass of B^0, it has many decay ways and the common way of the decays B^0 and $\overline{B}^0$ is rare. Belle and BaBaR has high luminosity around $5 \times 10^{33}\ cm^{-2}s^{-1}$ and so produce many B^0 mesons and the center of mass energy matches the mass of $\Upsilon(4S)$ $(10.58GeV)$ resonance which decays mainly into $B^0\overline{B}^0$ and B^+B^- pairs. The e^+e^- colliding bunches are energy-assymetric, what allows the $\Upsilon(4S)$ move and so is possible to reconstruct the decays of B-mesons and find out their decay time.

There are also transitions to change the B^0_q to antimeson $\overline{B}^0_q$ and conversely by exchanging W bosons between the b quarks and so the quark content is changed. See Fig. 2.4. The sum over all possible three coupling constants lead us to the unitary triangle which belong to the mixing process as in the picture 2.1. The strenght of the diagram is proporsional to the $mass^2$ of the objects which are in the middle and it happens that the top is very very heavy. Due to the large top mass both oscillations $B^0_q - \overline{B}^0_q$ dominated by this quark exchange. The V_{ts} has one power of λ less than the V_{td}. Moreover the frequency with which B mesons mix from one to another depends on the streght of the couplings. By the reason of that the coupling by the $B^0_d - \overline{B}^0_d$ mixing in bigger than the one by the $B^0_s - \overline{B}^0_s$ mixing system and the oscillation $B^0_d - \overline{B}^0_d$ is slower. From the figure 2.4 and the fact that the B^0 and $\overline{B}^0$ decay further to fermions we have there two different interfering quantum paths (amplitudes) for going directly from B^0 to final state and the second corresponds to the transformation B^0 to $\overline{B}^0$ which then decays to the same final state. Through the interference we can be sensitive to the complex phase also investigate the CP violation. Experimentally it is difficult to decide whether the state was B^0 or $\overline{B}^0$ at the time it decayed.The cleanest but hardest way is to identify the flavor reconstructing a particular exclusive decay channel. However, in the B system the branching ratios to any final state are small and the reconstruction efficiencies are low. The other way is to use as flavor indicator the sign of the lepton in the semileptonic decay like it is in the following decay.

2.2.1 Decay $B^0_d \rightarrow D^* l\nu$

BaBar is one of the experiment where the effect of CP violation by $B^0_d - \overline{B}^0_d$ mixing is measured for example with use of the decay $B^0 \rightarrow D^* l\nu$[1]. In this semileptonic decay is the D^{*-} reconstruct through its decay to $\overline{D}^0\pi^-$ and use the three $\overline{D}^0$ decay modes $\rightarrow K^+\pi^-\pi^0$ and $\rightarrow K^+\pi^+\pi^-\pi^-$. Since following relation between the decay weights $\Gamma(B^0)$ and $\Gamma(\overline{B}^0)$ is not

[1]By this notation $B^0_d \rightarrow D^* l\nu$ are mentioned decays $B^0_d \rightarrow D^{*-} l^+\nu$ and $\overline{B}^0_d \rightarrow D^{*+} l^-\overline{\nu}$ where l indicates leptons $\mu^\pm$ or $e^\pm$.

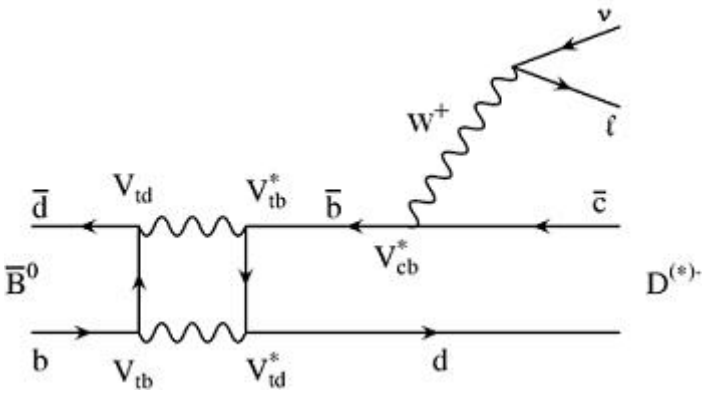

Figure 2.5: Feynman diagrams of $B^0_d \rightarrow D^{*-}l^+\nu$ decay.

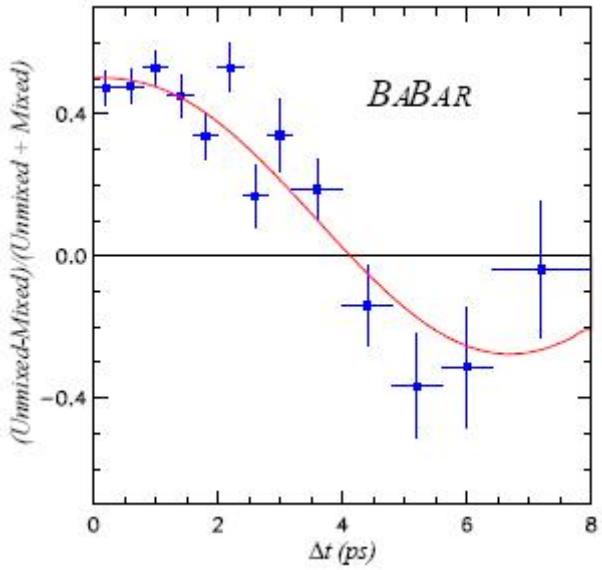

Figure 2.6: By BaBar measured time-dependence asymmetry between unmixed and mixed events for the $B^0 \rightarrow D^{*-}l^+\nu$ candidates.

equal to zero the CP has been violated:

$$\frac{\Gamma(B^0 \rightarrow D^{*-}l^+\nu) - \Gamma(\overline{B}^0 \rightarrow D^{*+}l^-\overline{\nu})}{\Gamma(B^0 \rightarrow D^{*-}l^+\nu) + \Gamma(\overline{B}^0 \rightarrow D^{*+}l^-\overline{\nu})} \neq 0 \tag{2.1}$$

This relation is time dependent and the amount of B^0, $\overline{B}^0$[2] mesons also by the decay processes oscillate like in the Figure 2.6. The oscillation frequency of mixing in this case was established like:

$$\Delta m_d = 0.508 \pm 0.020\,(stat.) \pm 0.022\,(syst.)\hbar\, ps^{-1} \tag{2.2}$$

This decay could be directly useful in order to measure $|V_{cb}|$ element of the CKM matrix which sets the length of the base of the unitarity triangle. Precise measurement of $|V_{cb}|$ relies

[2]In this case B^0 refers to B^0_d meson

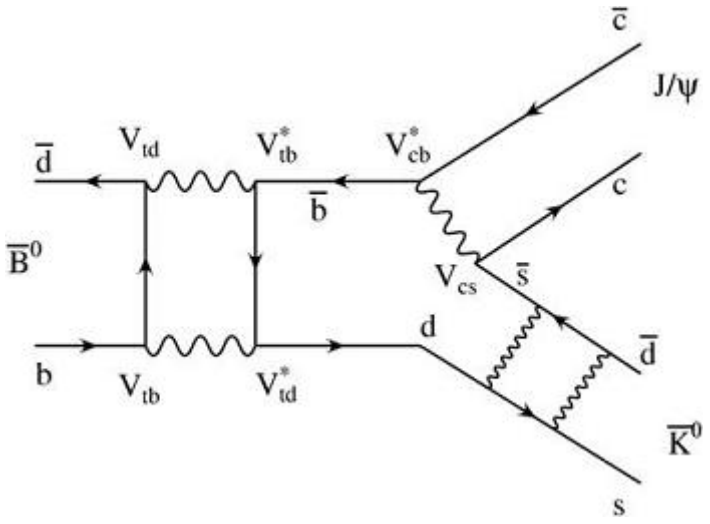

Figure 2.7: Feynman diagram of the golden decay $\overline{B}^0_d \rightarrow J/\psi \overline{K}^0_s$, where the $K^0 - \overline{K}^0$ is taken into account.

on the underlying quark decay $b \rightarrow cl\overline{\nu}$ and the experiment may focus on two possible ways of approach. The first approach combines measurements of the inclusive semileptonic branching fraction and lifetime to determine the semileptonic decay rate of the B meson, which is proportional to $|V_{cb}|^2$. The second method uses specific decay mode $\overline{B}^0_d \rightarrow D^* l\nu$ which rate depends on $|V_{cb}|$, weak decay physics and on strong interaction effects. These effects are difficult to quantify but thanks to b and c quark mass they can be treated by so called Heavy Quark Effective Theory (HQET) which exploits the theory of heavy-quark symetry.

Using a sample of 3×10^6 $B\overline{B}$ events in the CLEO detector at the Cornell Electron Storage Ring were meaured decay rates of the decay $\overline{B}^0_d$.The analysis done in CESR utilized the kinematic constraints available at the $\Upsilon(4S)$ resonance to suppress backgrounds.

The decay where electron arises gives value $|V_{cb}| = 0.0420 \pm 0.0023$ and for decay with muon $|V_{cb}| = 0.0448 \pm 0.0026$ (with statistical errors only).In present most exact value was obtained from many measurements as $|V_{cb}| = 0.0416 \pm 0.0006$.

2.2.2 Golden decay $B^0_d \rightarrow J/\psi K^0_s$ and measuring of $sin(2\beta)$ of unitary triangle

If one would like to measure the angle

$$\beta = arg\left(-\frac{V_{cd}V^*_{cb}}{V_{td}V^*_{tb}}\right) \tag{2.3}$$

of the unitary triangle in the picture 2.2 it is needful to find the process that involves the to the β corresponding CKM matrix elements. From the Feynman diagram 2.7 of the golden decay is obvious that we are not able to built the ratio like this $V_{cd}V^*_{cb}$ but this decay alone is proportional to $V_{cs}V^*_{cb}$. If we consider the B^0 meson mixing first defore it decays (see Figure 2.4) with the dominative top quark exchange, we see that this mixing is proportional to the $(V_{td}V^*_{tb})^2$ what is the second power of the denominator in the β definition. But K^0 and $\overline{K}^0$ are produced

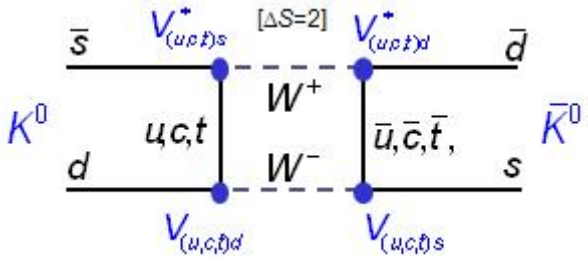

Figure 2.8: Feynman diagram of the $K^0 - \overline{K}^0$ mixing)

from the decays of B^0 and $\overline{B}^0$. Therefore for the interference of these processes must mix K^0. From the CKM elements mainly contributing to $K^0 - \overline{K}^0$ mixing see picture 2.8 is this mixing proportional to $(V_{cd}V_{cs}^*)^2$.

Now is possible to theoretically put all the decays together to obtain the angle β. First B^0 transforms to $\overline{B}^0$ then it decays into $J/\psi\overline{K}^0$ which ($\overline{K}^0$) then transforms to K^0 :

$$arg\left[\frac{Amplitude(B_d^0 \rightarrow J/\psi K_s^0)}{Amplitude(B_d^0 \rightarrow \overline{B}_d^0 \rightarrow J/\psi\overline{K}_s^0 \rightarrow J/\psi K_s^0)}\right]$$

$$= arg\left[\frac{V_{cs}V_{cb}^*}{(V_{td}V_{tb}^*)^2 V_{cs}^* V_{cb} (V_{cd}^* V_{cs})^2}\right] = arg\left[\frac{(V_{cd}V_{cb}^*)^2}{(V_{td}V_{tb}^*)^2}\right] = -2\beta$$

[3] We would like to determine something as follows:

$$Amplitude(t) = \frac{\Gamma(\overline{B}^0(t) \rightarrow J/\psi K_s) - \Gamma(B^0(t) \rightarrow J/\psi K_s)}{\Gamma(\overline{B}^0(t) \rightarrow J/\psi K_s) + \Gamma(B^0(t) \rightarrow J/\psi K_s)} = sin(2\beta) \cdot sin(\Delta m_d t) \tag{2.4}$$

,where Δm_d is the oscillation frequency (like the one by B^0 mixing mentioned above). If one would like to make an experiment it is essential to identify our final CP eigenstate $J/\psi K_s$ and to determine the flavour of decaying B^0. There exist an **Einstein-Podolsky-Rosen phenomenon** which tells that if we produce two coherent quantum states (synchronous evolution of $B^0\overline{B}^0$ - mixed state) the measure of the flavor (or CP) of one meson (e.g. in this case from its decay products which is not the CP eigenstates) determines the flavor (or CP) of the other meson at the same proper time (it is opposite). Once the coherence is destroyed by the decay of one B^0 we need the decay time difference between the two B^0's to calculate the flavour of the tagged B^0 at the time when the second B^0 decayed. The BaBar and Belle factories use above mentioned electron-positron assymetry-energy bunches to determine these relative decay times of the B^0's from $\Upsilon(4S)$ decay by measuring their decay vertices. Concretely the example of B-tagging in BaBar factory is shown in the Figure 2.9. So we need to know which of B^0,$\overline{B}^0$ decayed in the final state $J/\psi K_s^0$. This decay we find for example with cuts on the reconstructed invariant masses of $J/\psi \rightarrow \mu^+\mu^-$ and $K_s^0 \rightarrow \pi^+\pi^-$. If we found for example some lepton or charged kaon we are able to identify the flavour of the B_{tag} before it decays to them and also in the same time we know the flavour of B_{rec}. Now we take the oscillation frequency for $B^0 - \overline{B}^0$ mixing and with use of the tiny time difference between the decays of B_{tag} and B_{rec} received from

[3] We can assume that the higher quantum contribution (loop/penguin diagrams) are very small.

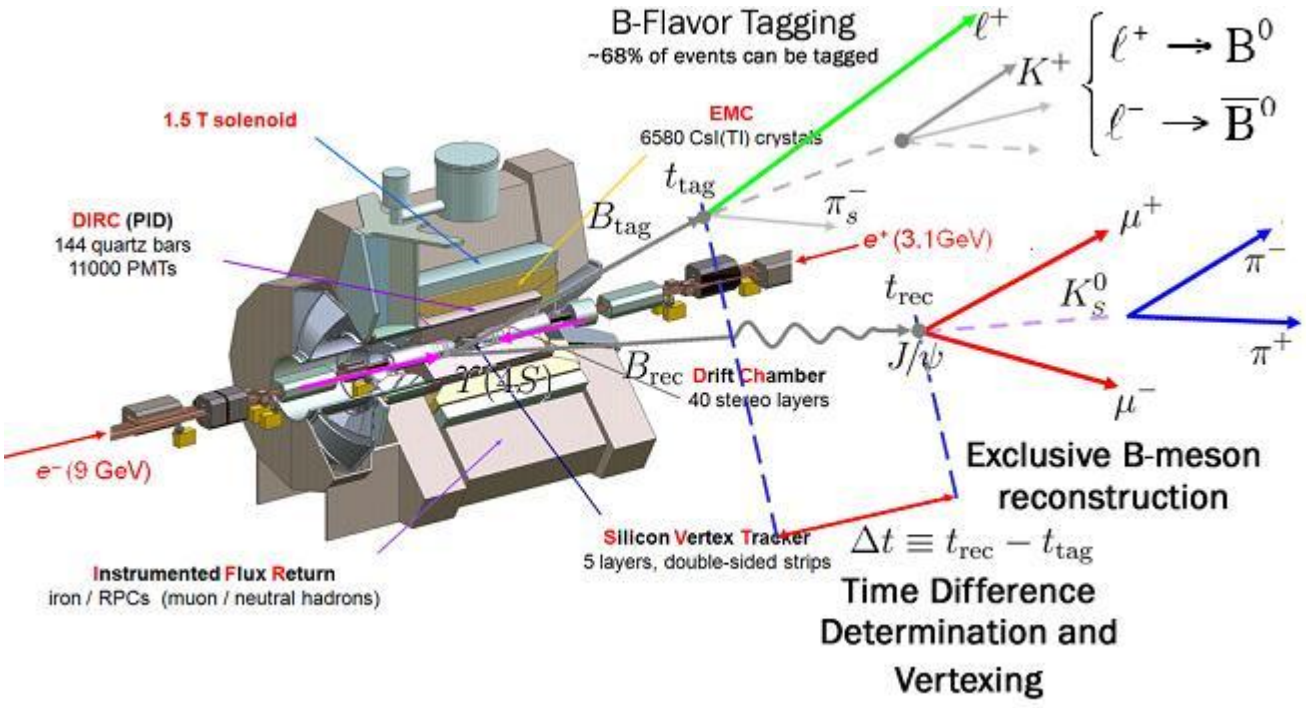

Figure 2.9: Brief description of BaBar factory and example of B^0- flavour tagging

vertexing (we know speed of B_{rec}, we may fix the flavour of the B_{rec}. Conceptually we try to measure the CP violation due to the interference of decays B^0, $\overline{B}^0$ with and without mixing. Precise measurements gives us $\mathbf{sin(2\beta) = 0.687 \pm 0.032}$.

2.3 By me analysed decay $B^+ \rightarrow J/\psi K^+$

Decay I am going to describe was observed mainly in many experients at BaBar(SLAC) and BELLE (KEK). It is a methodical channel because from these measurements we already know much about this decay. The branching ratio of this decay still now has been fitted as the value of $= \ (10.08 \pm 0.35) \times 10^{-4}$. It is as well important reference channel in the view of the first ATLAS data i.a. for example as the control channel for the CP violation studies, too. New channels e.g.: $(B \rightarrow \mu\mu)$will be measured relative to this and one of the tasks is to determine more exactly the B^+ mass, lifetime and differencial cross section. We expect about 17 000 events of this type during 1 year of running the ATLAS experiment at luminosity of $10^{34}\ cm^{-2}s^{-1}$.

The ATLAS offline analysis objects allow to write object oriented analysis code in Athena (see Chapter 5) using AOD (Analysis Object Data) files. The standard tools supplied B-physics group with additional tools as vertex fitters, track manipulation utilities ,etc.. For analysis of the decay $B^+ \rightarrow J/\psi K^s+$ was developed a code in Athena which I used for my analysis. The code could be found on the server lxplus.cern.ch at /afs/cern.ch/user/g/guenther/public and the data I used are AOD files from full chain Monte Carlo production stored at CASTOR see 5. This code operates according to the user's requirements in job options pythia file in principle as follows. First we try to find some J/ψ which we suppose decays further into $\mu^+\mu^-$. The Muon

candidates can be identified using the information from the analysis object called 'MuonContainer' or by using only kinematic cuts and so are formed all possible unique oppositely charged pairs of muon candidates. Track pairs which are retained after the p_T - transverse momentum cut (one with $p_T \geq 6\,GeV$ and one with $p_T \geq 3\,GeV$) are then fitted to a common vertex using the CDF fitter with the mass constrained to $m_{J/\psi}$. Where the χ^2 per degree of freedom [4] and the transverse decay length $l_{xy} \geq 0.1\ mm$ (corresponds with the proper decay time $= 0.5\ ps$ of the B^+) of the vertices pass the cuts provided in the job options, the vertices are accepted. Considered for J/ψ particles are only those J/ψ vertices whose calculated invariant mass falls inside the window around J/ψ mass defined in the job options. Original collection of tracks is then scanned again (excluding denoted muon pairs) to thrown away tracks which does not fit the kinematic cuts in the job options and we keep the ones that have positive charge and are inconsistent with coming from the primary vertex . This way we obtained K^+ candidates. The pairs of muons are coupled with the K^+ into unique triplets and the tracks in each triplet are fitted to a common vertex (it is assumed that the decay length of the J/ψ is negligible, such that the three tracks originate from one point). The momentum vector of the vertex is required to point at the primary vertex, and the two muon tracks are again constrained to $m_{J/\psi}$. And again with reference to the cuts of χ^2 per degree of freedom the transverse momentum and the transverse decay length l_{xy} of the vertices in the job options, the vertices are chosen. Finally is calculated the invariant mass of all previously accepted vertices and those whose invariant mass falls inside the window around B^+ mass defined in the job options are accepted and denoted as B^+ mesons and the output file is created.

2.3.1 Invariant Mass of J/ψ and B^+ received from the analysis of the decay:

$B^+ \rightarrow J/\psi(\mu^+\mu^-)K^+$

I used the BPlus.cxx code written by Christos Anastopoulos to analyze this decay channel. By me used cuts (job options file) as well as all other files used in the analysis could be seen on the LxPlus server at /afs/cern.ch/user/g/guenther/public. Also the athena analyse the example events and write the results to an Athena-Aware NTuple file which I inspected with ROOT. I had to write a ROOT code for working with this file to receive the histogram of the invariant mass of the J/ψ and B^+ from muon pairs see Figure 2.10; 2.11; 2.12. The width of the fitted gauss distribution is larger than it should be in reality by reason of the detector multiple scattering effects. The tails at the edges of the histograms were not possible to be fitted by gauss, because they originate from muon energy loss along its track.

Comments to the decay $B^+ \rightarrow J/\psi(e^+e^-)K^+$

The J/ψ could decay into $\rightarrow\ e^+e^-$ pairs. If one would like to compute the histogram of the invariant mass of J/ψ from these electron-positron pairs it could be expected that the width of the fit is larger because electrons lose its energy along the trajectory due to bremsstrahlung. I code for this analysis in unfortunately still not written, and I do not have so much time to participated on its development. But from the consultation about J/ψ invariant mass reconstruction

[4] χ^2 is standard parameter of approach to fitting vertices and it has to do with the quality of the fit

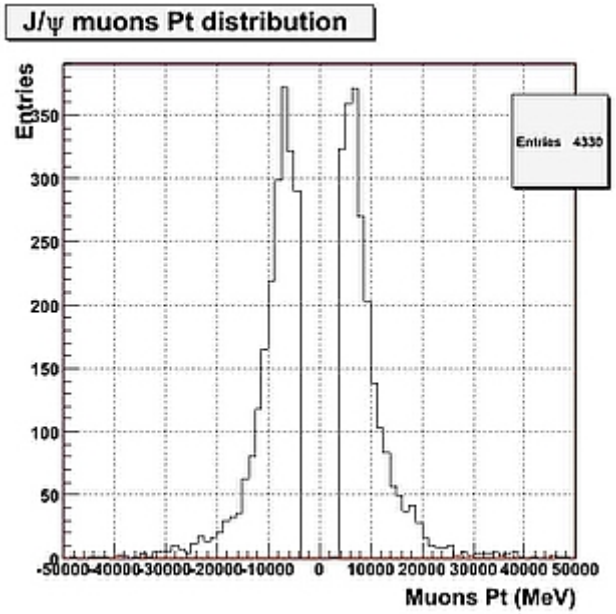

Figure 2.10: The J/ψ muons p_T distribution. Opposite sign in p_T means negative positive charge.

5

from electron positrom pairs ensue that basically it is true that with muons we may have better results, as efficiency of reconstruction is better and resolution also, but still it might be good for an analysis to have one more approach by using electron decays. Moreover is this code important due to more reasons. Who knows what will come with first ATLAS data ? To do the muon chambers alignement etc. will take some time and for the analysis could be electrons for a while more useful. In fact the main reason is that we are interested in all $X \rightarrow e^+e^-$ resonance to study the electron reconstruction and understand calorimeter and inner detector (parts of the ATLAS detector). If we will have low background, then the fact to have the resonance favours the use of these events to study the decay product (same stands for muon decays of course). For J/ψ you have a huge amount of data produced. For electrons (also for muons) you have the Z which is the first thing to look at in first data, but electrons and muons are of high transverse momentum. The J/ψ or Υ resonance because of their low mass give low p_T electrons (or muons), so we are able to study our favourite detector at lower energies, in particular check the energy scale. That is if the J/ψ or Z mass is well reconstructed at its known value. If not we have a way to calibrate the energies, and we can do it at different energies - not only with Z. Also we can intercalibrate our detector whether is the reconstructed J/ψ or Z mass the same everywhere in the detector. If not we can correct the inhomogenities. Finally at low energies is our sensitivity to the to the amount of material in front of the calorimeter much better.

Huge potential of rare heavy quark decays has LHC (Large Hadorn Collider - CERN) which e.g. on ATLAS should produce 5×10^{12} $b\bar{b}$ pairs per year and can detect B-decays with the branching ratio about $10^{-11} - 10^{-12}$.

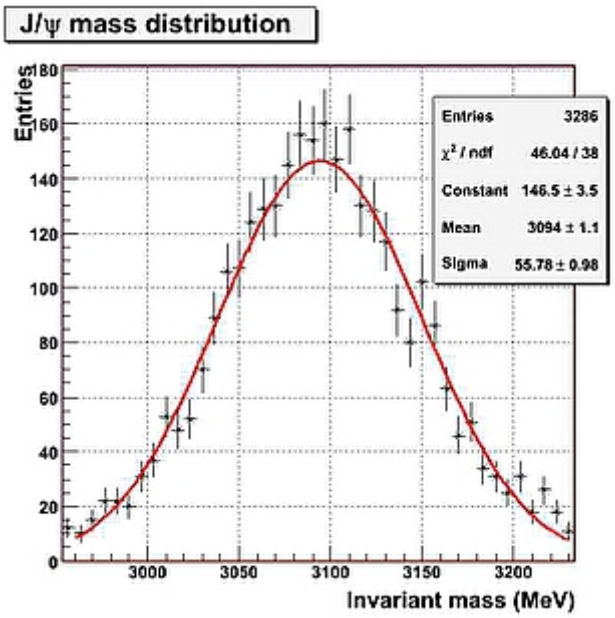

Figure 2.11: Invariant mass of J/ψ particle calculated from muon pairs p_T.

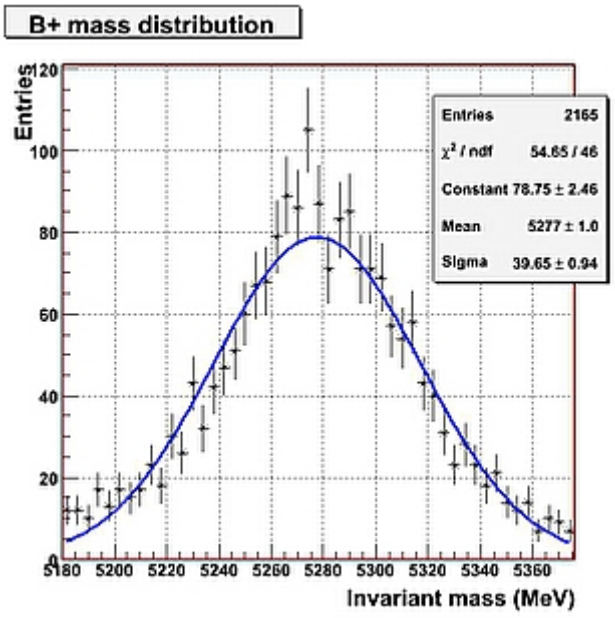

Figure 2.12: Invariant mass of B^+ particle.

Chapter 3

Planned Experimental Equipment, Basic Characteristic

3.1 Large Hadron Collider

The aim of the Large Hadron Collider (LHC) is to push our understanding of the fundamental structure of the universe. The main reason for the LHC experiment is to discover the Higgs boson and eventually supersymmetric particles if they exist. It is built in a circular tunnel which is buried from 50 to 175 m underground and has $26.659\ km$ in circumference. It straddles the Swiss and French borders on the outskirts of Geneva. The LHC will collide 7 TeV protons together with a centre of mass energy of 14 TeV and a design luminosity of $10^{34} cm^2 s^{-1}$. First beams are expected to run in May 2008 and first collisions at high energy are expected middle of 2008 with the first results from the experiments soon after. To control the beam are used 1232 superconducting dipole magnets 3.1 ensuring the differently oriented magnetic field in each pipe and so allow to run the same charged beams in opposite direction. Injected beam will increase from the energy $450\ GeV$ (protons) up to the beam energy at collision $7\ TeV$ and magnetic field at this full experiment potencial use will reach $8.33\ Tesla$ at operating temperature about $1.9\ K$. The fully-loaded revolution frequency may be 11.2455 kHz by power consumption $120\ MW$.

3.2 ATLAS

With a size similar to that of five stored building (see Figure 3.3) the **A** **T**oroidal **L**HC **A**pparatu**S**) is the largest-volume collider detector ever constructed which exploit the full LHC potential. More than 1800 scientists and engineers from 34 countries participate in this project. The main goals are except the search for the Higgs boson and supersymetric particles, the investigation of CP violation in B-decays as well as precise measurements of mass of heavy particles. Not least stands there the question, are fermions really fundamental ? To explore all the tasks the ATLAS consist of many components which are able to detect the whole amount of accessible information with respect to our today's technical ability. The ATLAS detector consists of four major components, the Inner Tracker which measures the momentum of each charged particle,

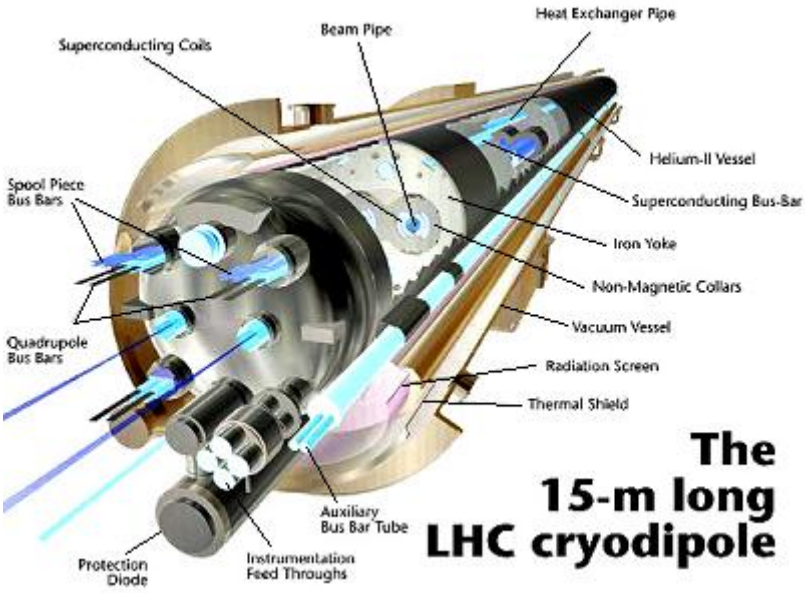

Figure 3.1: Many of the major components of one of the 15 m long superconducting magnets for the LHC at CERN.

the Calorimeter which measures the energies carried by the particles, the Muon spectrometer which identifies and measures muons and the Magnet system that bends charged particles for momentum measurement.

3.2.1 Inner Tracker

The ATLAS Inner Detector combines high-resolution detectors at the inner radii with continuous tracking elements at the outer radii. Around the vertex region is achieved the highest granularity using semiconductor pixel detectors followed by a silicon microstrip detector. The outer radius of the Inner Detector is 1.15 m, and the total length 7 m. In the barrel region the high-precision detectors are arranged in concentric cylinders around the beam axis, while the end-cap detectors are mounted on disks perpendicular to the beam axis. The barrel TRT straws are parallel to the beam direction. All end-cap tracking elements are located in planes perpendicular to the beam direction see picture 3.4.

Pixel Detector

Pixel Detector provides a very high granularity, high precision set of measurements as close to the interaction point as possible.The system determines the impact parameter resolution and the ability of the Inner Detector to find short lived particles such as B-Hadrons. One Pixel sensor is a $16.4 \times 60.8\ mm$ wafer (=module) of silicon with $46\,080$ pixels , 50×400 microns each. It consist of three cylindrical layers - barrels with the radial positions of $50.5\ mm$, $88.5\ mm$ and $122.5\ mm$ respectively. These three barrel layers are made of identical staves inclined with azimuthal angle of 20 degrees. There are 22, 38 and 52 staves in each of these layers respectively. Each stave is composed of 13 pixel modules. There are three disks on each side

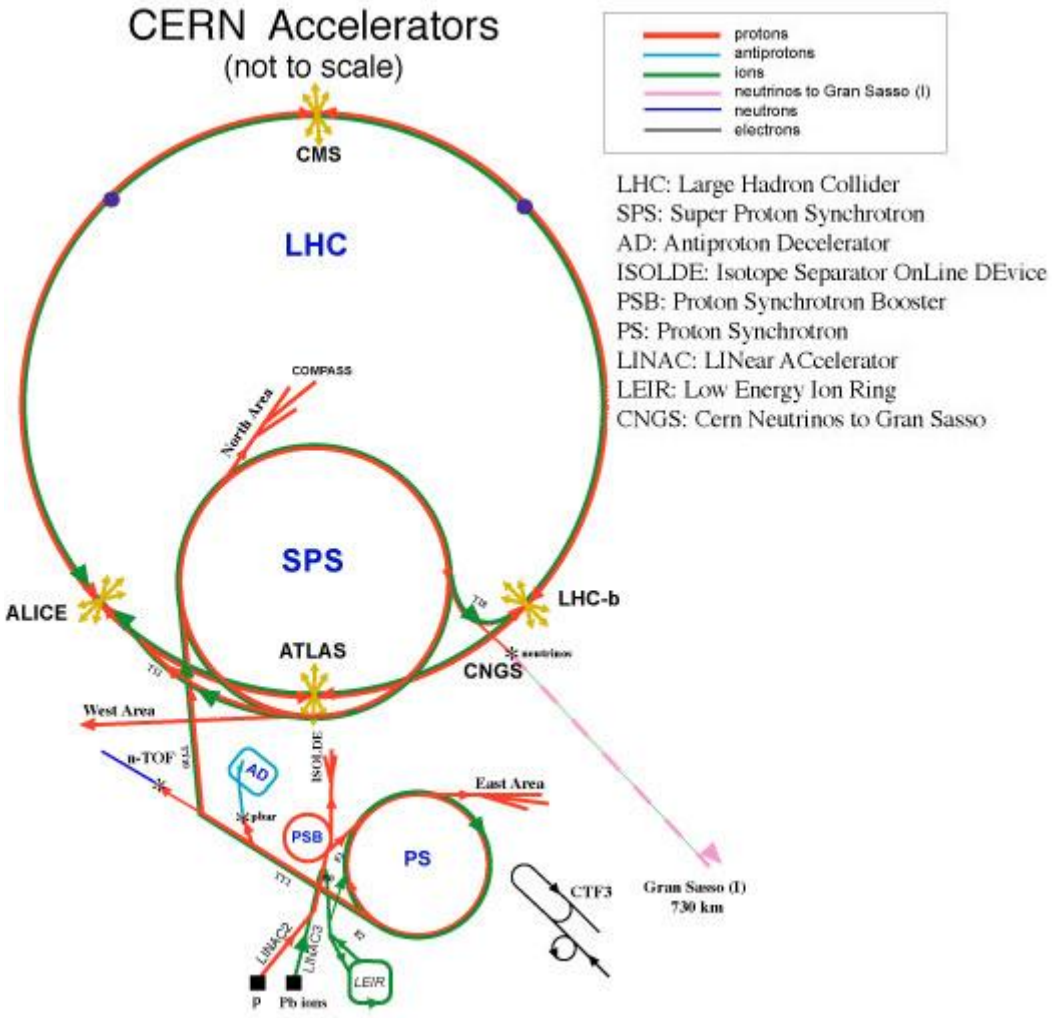

Figure 3.2: All of the LHC experiments with all the boosting rear.

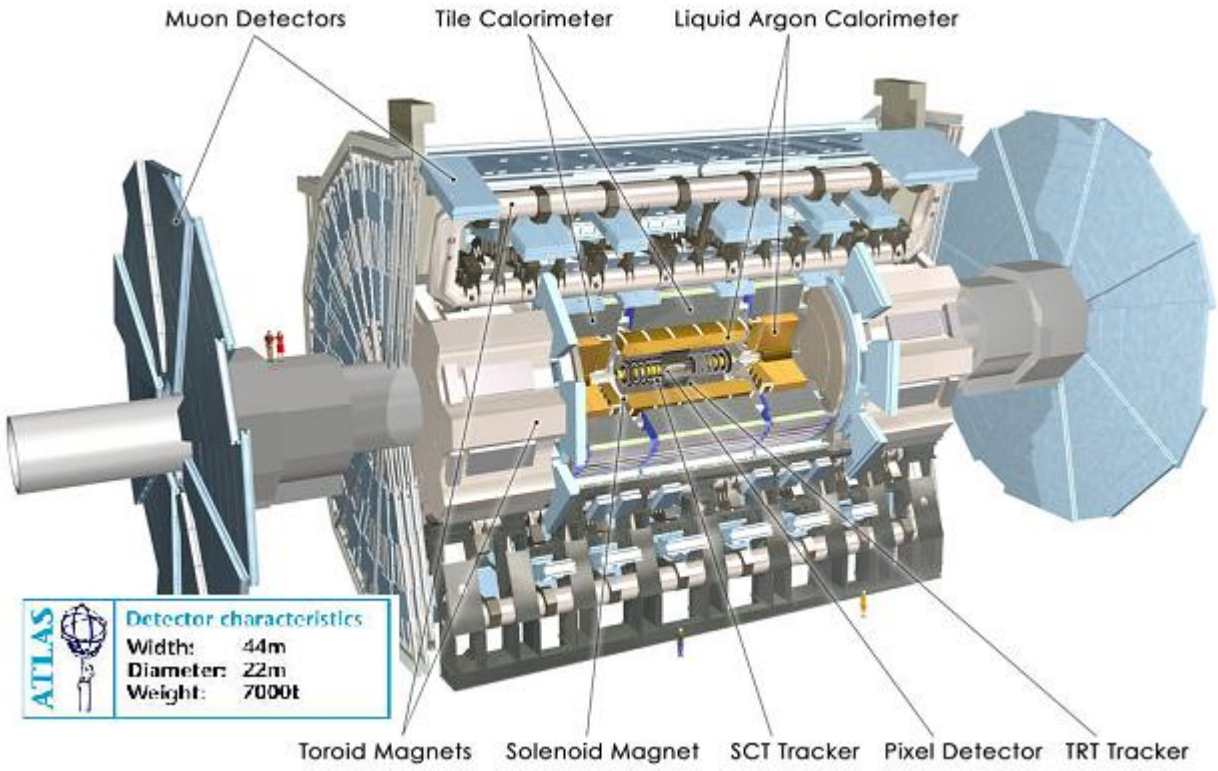

Figure 3.3: Look at the ATLAS detector.

of the forward regions. One disk is made of 8 sectors, with 6 modules in each sector. Disk modules are identical to the barrel modules, except the connecting cables. Each module will be read out by 16 chips, each serving an array of 18 by 160 pixels.

Semiconductor Tracker (SCT)

The SCT system is designed to provide eight precision measurements per track in the intermediate radial range, contributing to the measurement of momentum, impact parameter and vertex position. In the barrel SCT eight layers of silicon microstrip detectors provide precision points in the r-phi and z coordinates [1], using small angle stereo to obtain the z-measurement. Each silicon detector is $6.36 \times 6.40\ cm$ with 768 readout strips of 80 micron pitch. The barrel modules are mounted on carbon-fibre cylinders at radii of $30.0,\ 37.3,\ 44.7,$ and $52.0\ cm$. The end-cap modules are very similar in construction but use tapered strips with one set aligned radially. The SCT covers $|\eta| \prec 2.5$[2].

[1]The ATLAS coordinate system is a right-handed system with the x-axis pointing to the centre of the LHC ring, the z-axis following the beam direction and the y-axis going upwards. Φ is an azimutal angle

[2]Pseudorapidity $\eta = -log\left(tan\ \frac{\Theta}{2}\right)$, where Θ is an angle measured from the z axis.

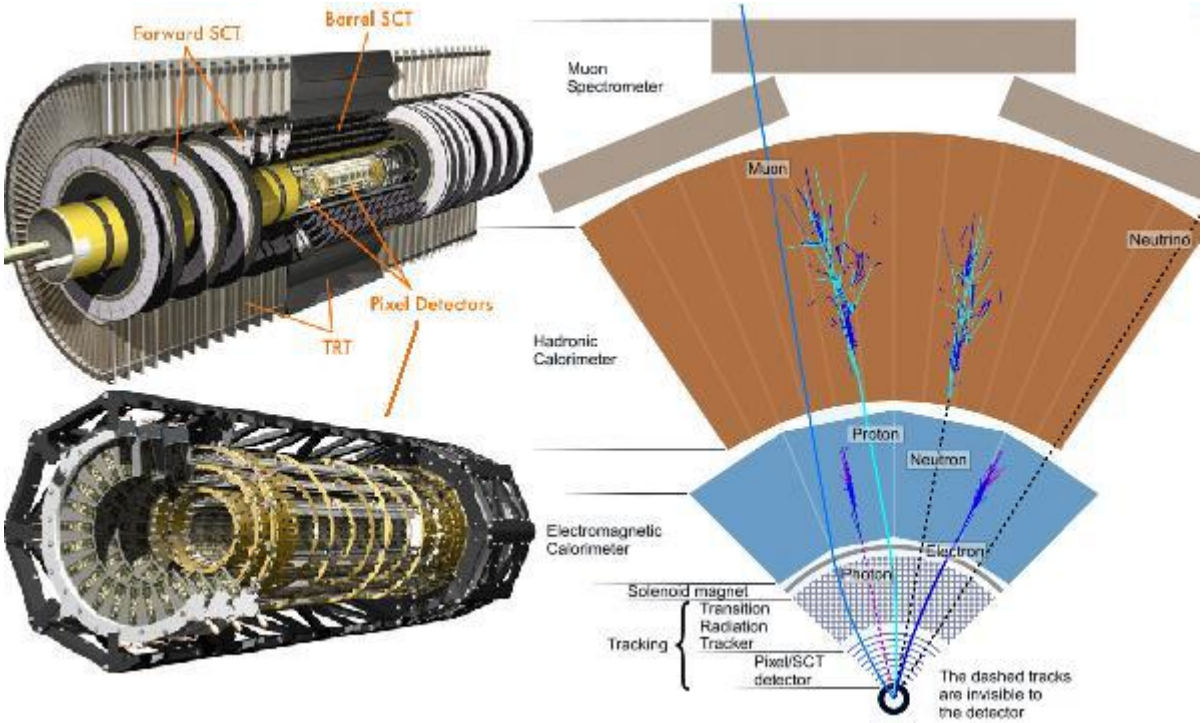

Figure 3.4: Layout of the Inner detector with basic scheme of particle identification.

Transition Radiation Tracker (TRT)

TRT) is based on the use of straw detectors, which can operate at the expected high rates due to their small diameter and the isolation of the sense wires whitin individual gas volumes. Electron identification capability is added by employing Xenon gas to detect transition radiation photons created in a radiator between the straws. Each straw is 4 mm in diameter and equipped with a 30 m diameter gold-plated W-Re wire. The maximum straw length is is 144 cm in the barrel, which contains about 50 000 straws, each divided in two at the center and read out at both end, to reduce the occupancy. The end-caps contain 320 000 radial straws, with the readout at the outer radius. The total number of channels that are read out is 420 000. Each channel provides a drift time measurement, giving a spatial resolution of 170 m per straw, and two independent thresholds. These allow the detector to discriminate between tracking hits, which pass the lower threshold, and transition radiation hits, which pass the higher one.The barrel section is built of individual modules between 329 and 793 straws each, covering the radial range from 56 to 107 cm. The first six layers are inactive over the central 80 cm of their length to reduce their occupancy. Each end-cap consists of 18 wheels. The innermost 14 cover the radial range from 64 to 103 cm, while the last four extend to an inner radius of 48 cm. Wheels 7 to 14 have half as many straws per cm in z as the others, to avoid an unnecessary increase of crossed straws and material at medium rapidity.

3.2.2 Calorimeter

Liquid Argon Calorimeter

The Liquid Argon (LAr) Calorimeter is divided into several components: an electromagnetic sampling calorimeter with 'accordion-shaped' lead electrodes in the barrel and in the endcaps, a hadronic calorimeter using at copper electrodes in the endcaps, and a forward calorimeter close to the beampipe in the endcap made from copper and tungsten. In addition, presamplers consisting of one layer of LAr in front of the electromagnetic calorimeter help to correct for the energy loss in front of the calorimeter (mainly due to cryostat walls and the barrel solenoid).

Tile Calorimeter

The Tile Calorimeter is a large hadronic sampling calorimeter which makes use of steel as the absorber material and scintillating plates read out by wavelength shifting (WLS) fibres as the active medium. It covers the central range $|\eta| \prec 1.7$. The new feature of its design is the orientation of the scintillating tiles which are placed in planes perpendicular to the colliding beams and are staggered in depth. A good sampling homogeneity is obtained when the calorimeter is placed behind an electromagnetic compartment and a coil equivalent to a total of about two interaction lengths of material. The Tile Calorimeter consists of a cylindrical structure with an inner radius of $2280\ mm$ and an outer radius of $4230\ mm$. It is subdivided into a $5640\ mm$ long central barrel and two $2910\ mm$ extended barrels as shown in the Figure below. The thickness of the calorimeter in the gap is improved, which has the same segmentation as the rest of the calorimeter. The total number of channels is about 10000.

3.2.3 Muon Spectrometer

In the barrel region ($|\eta| \prec 1.0$), which is covered by the large barrel toroid system, muons are measured in three layers of chambers around the beam axis using precision Monitored Drift Tubes (MDTs) and fast Resistive Plate Chambers (RPCs). In regions of larger pseudorapidity, also three layers of chambers are installed, but vertically. Here Thin Gap Chambers (TGCs) are used for triggering. The precision measurement of muons is again done with MDTs, except for the innermost ring of the inner station of the end caps and for $|\eta| \succ 2$, where high particle uxes require the more radiation tolerant Cathode Strip Chamber (CSC) technology. In the barrel of the ATLAS muon system, the muon chambers are installed in three cylinders concentric with the beam axis at radii of about 5, 7.5 and $10\ m$. They are arranged to form projective towers pointing to the nominal interaction vertex. In the end caps, the distance in z from the vertex is about 7, 10 and $14\ m$ for the three layers.

3.2.4 Magnet system

Central Solenoid

The central ATLAS solenoid has a length of $5.3\ m$ with a bore of $2.4\ m$. The conductor is a composite that consists of a at superconducting cable located in the center of an aluminum stabaliser with rectangular cross-section. It is designed to provide a field of $2\ T$ in the central tracking volume with a peak magnetic field of $2.6\ T$. To reduce the material build-up the solenoid shares the cryostat with the liquid argon calorimeter.

Toroid Magnet

The ATLAS Toroid Magnet system consists of eight Barrel coils housed in separate cryostats and two End-Cap cryostats housing eight coils each. The End-Cap coils systems are rotated by 22.5^0 with respect to the Barrel Toroids in order to provide radial overlap and to optimise the bending power in the interface regions of both coil systems.

3.3 CMS

The **C**ompact **M**uon **S**olenoid) is similarly to ATLAS a general purpose detector optimized for tracking muons. Therefore it has alike goals. In addition CMS will try to study heavy ion collisions and the formation of the quark-gluon plasma. Through this CMS wants to approach closer to the very first moments after the Big Bang. CMS is a little bit smaller than ATLAS but has about twice its weight. Its magnet is the largest solenoid ever built, producing a magnetic field of the strength of 4 Tesla.The solenoid magnet is $13\ m$ long and $6\ m$ in diameter, and its superconducting niobium-titanium coils carry 20 kA at a temperature of 4.2 K. 2000 scientists and engineers from 36 countries collaborate on CMS project. The two construction ways in building ATLAS and CMS stands there to independently confirm the results flowing from the same physical phenomena. With this we try to reduce systematic as well as random errors.

The first detector inside the solenoid is the hadron calorimeter (HCAL), which measures the energy of hadrons and consist of layers of brass embedded with plastic scintillator. The next hadron detectors, located at the ends of the overall detector outside the magnetic volume, use quartz fibres embedded in steel wedges to measure very high energy forward-going particles. The electromagnetic calorimeter (ECAL) detects and measures the energies of electrons and photons, and fits within the HCAL. It will ultimately contain some 76 000 lead-tungstate scintillating crystals. The inner tracking system forms the heart of the CMS and is designed for precise measurement of the momentum of charged particles. About 210 m^2 of silicon microstrip detectors provide the required precision in the bulk of the tracking volume while pixel detectors are used close to the interaction region where the density of tracks is highest [35].

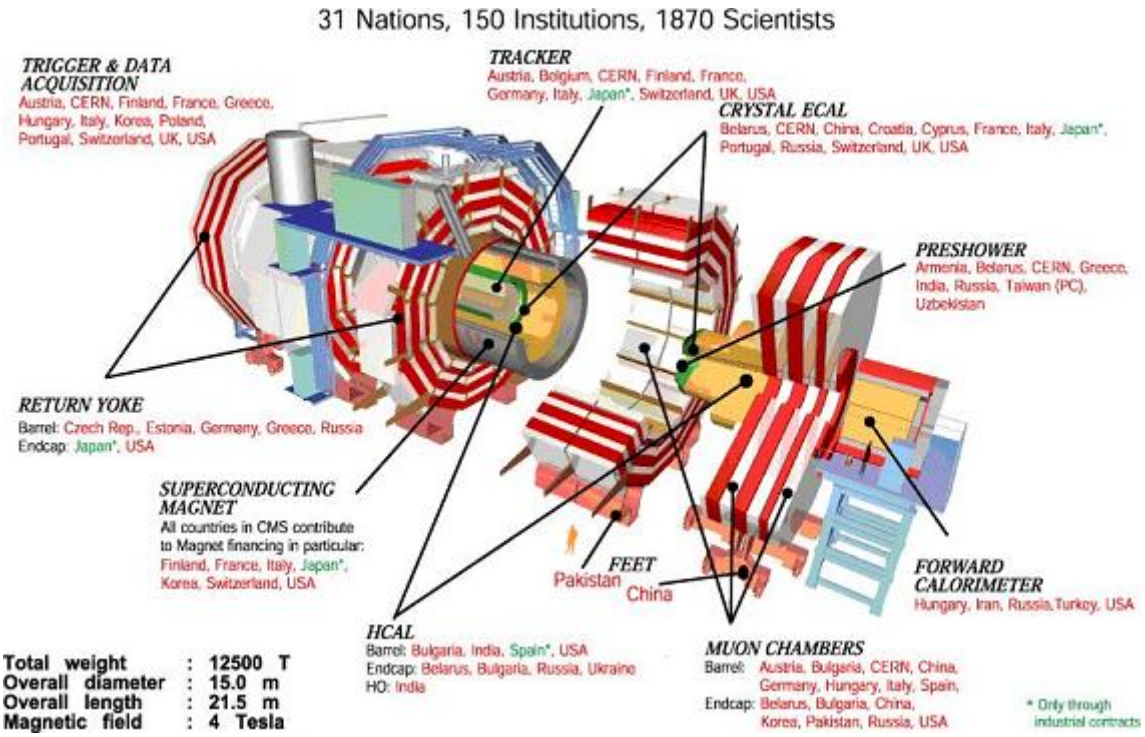

Figure 3.5: Description of the CMS detector.

3.4 ALICE

The (**A** **L**arge **I**on **C**ollider **E**xperiment) is a detector designed to study strongly interacting matter and the quark-gluon plasma - a new state of matter in collisions of heavy ions. Why we deal with the new state of matter ? Since there was shown that at very high temperatures the quarks are not confined inside hadrons but they are rather free in a state which was called the quark-gluon plasma (QGP). The prove of its existence provides experiments in the CERN in 1990's and in the Brookhaven National Laboratory USA in 2000's. This state of matter may is naturally present inside the quasars and it was also one of the initial stages of the Universe. QGP will produce by colliding nuclei of lead with an energy of $5.5\,TeV$ per nucleon. Production of strange particles and the suppression of the production of J/ψ mesons may lead us directly to the QGP identification, because the turmoil of QGP prevents forming of heavy quark pairs. ALICE experiment has more than 1000 participants from 28 countries.

The central part of the detector measure hadrons, electrons and photons and a small-angle spectrometer is there placed to measure muons. This part is embedded in the large solenoid magnet used perviously in the L3 experiment at LEP (Large Electron-Positron collider). It is made up of an inner tracking system (ITS) of high resolution silicon detectors, a cylindrical time projection chamber (TPC) for momentum measurement, and a particle identification system. An array of scintilators on top of the L3 magnet will be used to trigger on cosmic rays. The muon spectrometer, which is shielded by several metres of material that absorbs most particles other than muons, consist of a dipole magnet to bend the trajectory of the muons and a set of detectors to sample the tracks. The trigger system plays a crucial role in the performance of the ALICE detector. It consist of two independent parts: a central trigger processor providing the trigger decision logic and a trigger distribution network that generates triggers for the readout

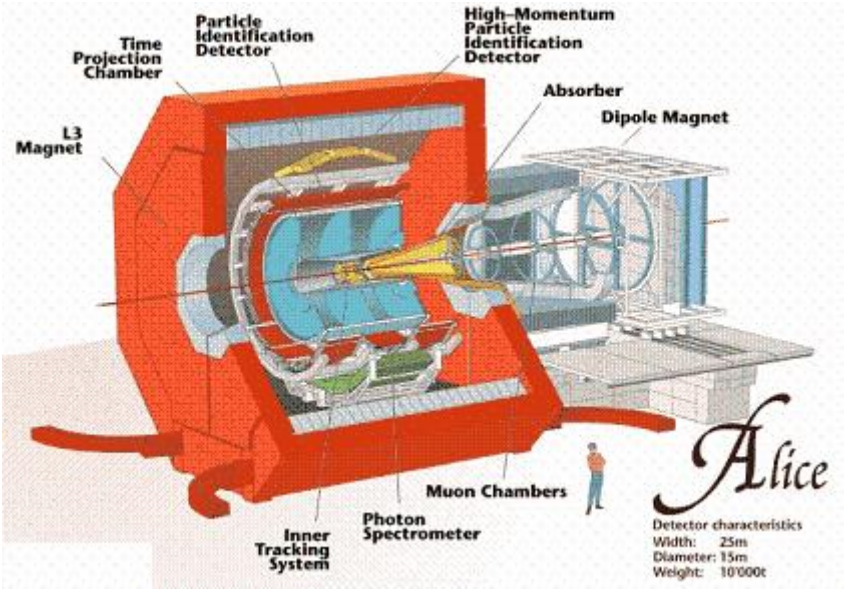

Figure 3.6: Layout of the ALICE detector.

by evaluating inputs from triggering detectors [34].

3.5 LHCb

The (**L**arge **H**adron **C**ollider **b**eauty) experiment aims to investigate fully the asymmetry between matter and antimatter in decays of B-particles. Especially we are sensitive to CP violation and CKM complex phase with $B_d - \overline{B}_d$ meson mixing decays in above mentioned 'golden decay'. None of the similar experiments before (LEP, SPS) did produce satisfactory number of b quarks to see clearly the CP violation effect.The LHCb collaboration involves nearly 900 people from 13 countries.

The LHCb magnet has a distingtive funnel shape, designed to capture of the cone of particles that will pour from point of proton collision. This magnet system will consume $4.2\ MW$ of electrical power and therefore it needs powerful cooling system (cca $150\ m^3/hour$ of demineralized water cool the system). The reconstruction of particle tracks in LHCb relies on a multistage tracking system that includes a vertex locator, trigger tracker and inner and outer trackers. The first three detectors are made from silicon sensors, while the outer detector consist of 53760 straws, each $2.5\ m$ long. arranged in modules $5\ m$ long and $0.34\ m$ wide. Further there are implemented the RICH detectors see Figure 3.7. Their duty is to identify charged particles. Upstream detector RICH1 is composed of aerogel and gas radiator and the downstream detector RICH2 of a gas radiator only. The electromagnetic and hadron calorimetrs have total readout of 7420 channels [36].

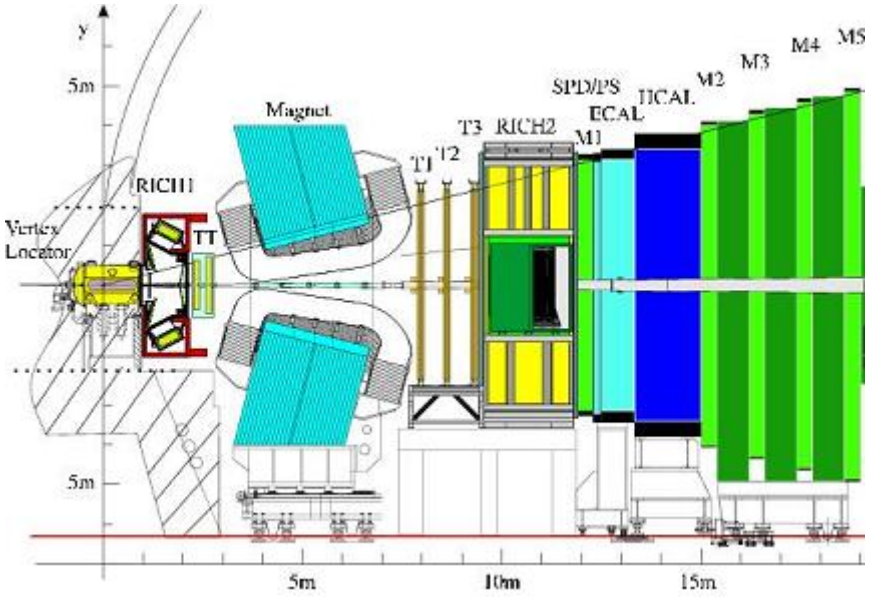

Figure 3.7: Layout of the LHCb detector.

Chapter 4

ATLAS Computing System

4.1 ATLAS Data Acquisition

In LHC will crossing over 2804 bunches (with approximately 10^{11} protons each) per beam with frequency 40MHz. We have to be able to select (almost) the most interesting bunches, collect all detector information for them and store it for an off-line analysis. Triggers with Data Acquisition system help us to online select the important events. This system operates by analogy to a photographer. All physics analysis runs off of the film (s)he produces. The particles after they cross flies with speed of $30\ cm/ns$ what with the fact that every $25\ ns$ 20 interactions happen implies that is needed to synchronize detector elements to better than 25 ns . Therefor fast response, high granularity ans radiation resistance, these are the mainly requirements on the detector design to try to explore the present physics. With respect to our ability to store data at $10^2\ Hz$ we must inspect detector information and provide a first decision on whether to keep the event or throw it out. The trigger is a function of time over that the system of triggers reduce the frequency of flow of the data from $40\ MHz$ to $10^2\ Hz$. There are 3 traditional physical level see Figure 4.1. At the Level-1 decision loop the trigger system decide only using the prompt data from calorimeter and muon detectors where for example in the Electromagnetic calorimeter the pattern recognition is much faster in contrast to the tracker info. There fore in the first stage are used only parts of the detector recognizing electrons, γ, jets, μ.

The technical specifications are indeed interesting see [38] but more complicated and it is not my intention to deal there with them more deeply. Finally are saveded the Event Summary Data (ESD) which stores calorimeter cells and tracking system hits thereby permitting many calibration and alignment tasks, but will be only accessible at particular computing sites with potentially large latency. In contrast, the Analysis Object Data (AOD) as the next step of the selection will contain a higher-level summary of the event data and will be more readily accessible for physics analysis. From the AOD, analysis can then produce more portable and customized derived physics data, which is ideally used for further analysis inside or outside Athena (see Section 4.2).

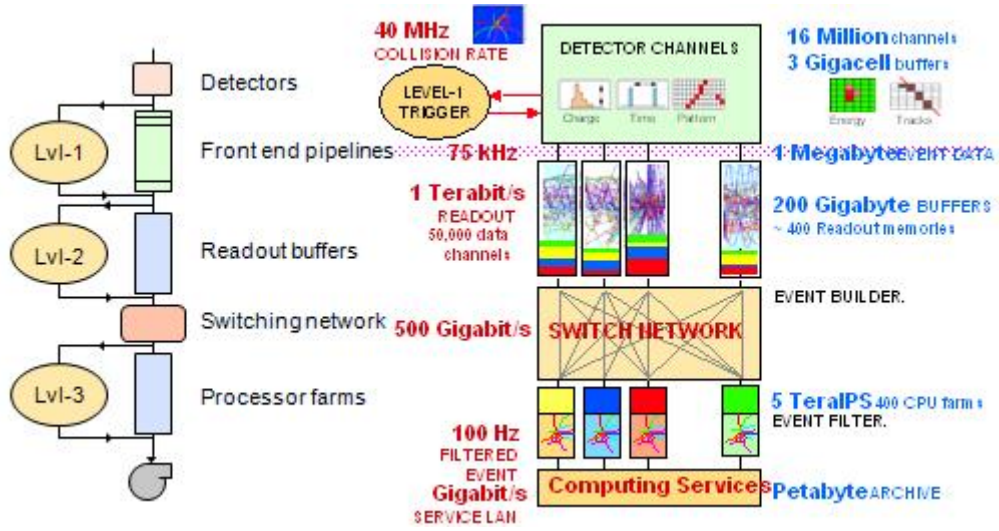

Figure 4.1: 3 levels of the online selection flow

4.2 Model of the ATLAS analysis

The ATLAS software for the analysis is ”packaged” into a control framework called ATHENA. The architecture of this framework covers all the abstraction objects and components and the way they interact with each other. Underlying Athena is the GAUDI architecture originaly developed by LHCb then with ATLAS collaboration (still in the progress) enhanced.[1]

In order to perform the analysis now still without the real data from the LHC experiment we produce the generated Monte Carlo events (with Pythia or Herwig generator for example). Then is simulated the response of our detector, digitized (this two steps could be done by Geant 4 for full reconstruction or Atlfast for quickly view [2]) then the event reconstruction algorithms have turn and reconstruct the event. From this stage this will done with the real data from the experiment. The produced ESD file (500kb/event) could be than with Athena summarize to an AOD file (100kb/event). The user analysis has than two stages. The first one is the Athena framework analysis, where we can select or remove objects by writing an Athena algorithm (C++ language). Find particles with some invariant mass cuts or derive other physics data as in the section 2.3. In the second stage we do out of framework analysis. It means we use ROOT for analyze and plot histograms etc. Almost everything about Athena could be found in by me used well written paper [41]. Now I would like only introduced the important components and tools which can be used by the analysis without deeply description since this is given in a very good references at the end of this thesis.

- ROOT is an object-oriented framework in which we can write scripts little bit similar to the C++ programming. Since it is a framework there are provided services and macros to use directly. ROOT is important tool to solve the data analysis challenges of high energy physics experiments. It provides a wide variety of objects like histograms, fitting scripts, etc. Only the basic knowledge of C++ programming and little experience should suffice

[1]The Gaudi is an open experiment independent project for providing the necessary interfaces and services for building frameworks in the domain of event data processing applications.

[2]Geant 4 is a toolkit for the simulation of the passage of particles through matter

to the physicists to write a code and analyze the data. The often used dokumentation is available at [42]

- Pythia

  PYTHIA is a program for the generation of high-energy physics events, i.e. for the description of collisions at high energies between elementary particles such as e^+, e^-, p and $\overline{p}$ in various combinations. Together they contain theory and models for a number of physics aspects, including hard and soft interactions, parton distributions, initial and final state parton showers, multiple interactions, fragmentation and decay. They are largely based on original research, but also borrow many formulae and other knowledge from the literature. This description has been taken from [40]

- Atlantis

  This very nice tool aimed to display events happened in the ATLAS detector.The primary goals of the program are the visual investigation and the understanding of the physics of complete events. Secondary goals are to help develop reconstruction and analysis algorithms, to facilitate debugging during commisioning and to provided a tool for creating pictures and animations for publications, presentations and exhibitions. This and much more information may be found at [39]

Chapter 5

GRID computing

5.1 Introduction

In case of some collecting experimental data e.g. suppose above mentioned CERN experiments, the data must be stored, analyzed etc. Earlier in the past all the data was stored in one processing center - CERN and for some simulations done at another equipment the data on tapes had to be transported manually. The software rear was written in Fortran. Nowdays when we are closer to the initial run of the LHC it has been required to have software written on the C++ basis and store the data in many different places due to their large size. For instance the estimation of the measured amount of the data only from ATLAS experiment is reaching $10^6\ GB/1\ year$, ($2\ PB/year$ for whole LHC). The system for processing all of this should know where the data are stored, where the job is optimal to perform as well as it should provide interactive access to all the data related to the appropriate experiment. So we need a **grid computing** as the distributed computing that involves coordinating and sharing computing, application, data, storage, or network resources across dynamic and geographically dispersed organizations. Or as Ian Foster said : "Grid is coordinated resource sharing and problem solving in dynamic, multi-institutional virtual organizations." Or "On-demand, ubiquitous access to computing, data, and services." We need to be able to don't care who owns resources, or where they are only they have to be able to be used by any authorizes person and users programs have to run there. In this concept does not exist any centralized control of resources or users.

For an example the LHC project requires a computing power equivalent to around 100000 of today's fastest PC processors. Since CERN can provide only aroung 20% of the capacity we had to start with solution called Worldwide LHC Computing GRID (WLCG). WLCG depends on two major science federations of independent GRIDs as infrastructures provided by Enabling Grid for E-SciencE (EGEE $\approx$ 160 communities) and US Open Science Grid (OSG). EEGE provide maybe 5PB storage and around 24000 processors in 40 countries. Aim of the next section is give survey of LCG Resources Distribution with a view to ATLAS experiment .

5.2 LCG Resources Distribution

Almost all of nearly 200 sites LCG sites support so-called ATLAS-VO. [1] LCG sites has split architecture. They are on the first level divided into 'Tiers' (further denoted by T0,T1... only). The foremost center is the T0 the accelerator centre - CERN where are swift produced Event Summary Data (ESD) and Analysis Object Data (AOD) - the first steps data acquisition and initia processing of raw data which then are distributed to the different Tier's. T1 includes 11 centers to the further online data acquisition process - re-reconstruction of raw data and producing new ESD, AOD. Also high availability of good managed mass storage elements for almost synchronous data-heavy analysis is required. Moreover each T1 support between 3 and 6 T2s for Monte Carlo simulations, end-user analysis etc. The other Tiers serves as opportunistic resources.
ATLAS counts 10 T1's (CNAF, PIC, SARA, RAL, BNL, TRIUMF, SINICA, LYON, FZK, NorduGrid) and of course T0 CERN.

- The ATLAS sites have been divided in CLOUDs which are : T0 (CERN), IT (Italy), ES (Spain), UK (United Kingdom), FR (France), CA (Canada), TW (Taiwan), DE (Germany), NL (Nederland)
- Every task in the ATLAS Production System is assigned to a specific cloud where jobs are running only in one of the cloud computing element (CE). Input data are fetched from one of the cloud storage elements (SE) and so the output data are stored only in one SE of the cloud.

All the prompts and commands I use for an example are commands I putted into the command line under operating system Linux using lxplus server as my user interface.

5.3 gLite - middleware for GRID computing

As gLite is called the middleware for grid computing born as a part of the EGEE Project. gLite provides a best-of-breed framework for building grid applications tapping into the power of distributed computing and storage resources across the Internet. As lately as we have an certificate from our certification authority (for Czech Republic i.e. CESNET) and as we are registered in ATLAS VO we could be able to use the GRID. Then with use of this certificate we may to initialize the proxy and start to work. gLite middleware is deployed through different elements see 5.1. Except the user interface (UI) where we can define our job by writing a JDL (Job Description Language) file is there resource broker (RB) where the job is submitted and sended on the GRID. RB keeps track of the job and notifies the Logging and Bookkeeping element (LB) about every change in status of the job. In order to find the best computing element (CE) matching the job requirements the RB parses the JDL and queries the BDII. (By the way BDII where the information about LCG resources is updated each 1-3 minutes.) The CE then submits the job and sends it to one of the underlying Worker Nodes (WN). The job at its end writes its output files to a storage element (SE) and in case of successful running they

[1] Users belonging to ATLAS Virtual Organization are able to read the ATLAS files or to exploit resources reserved to the ATLAS collaboration.

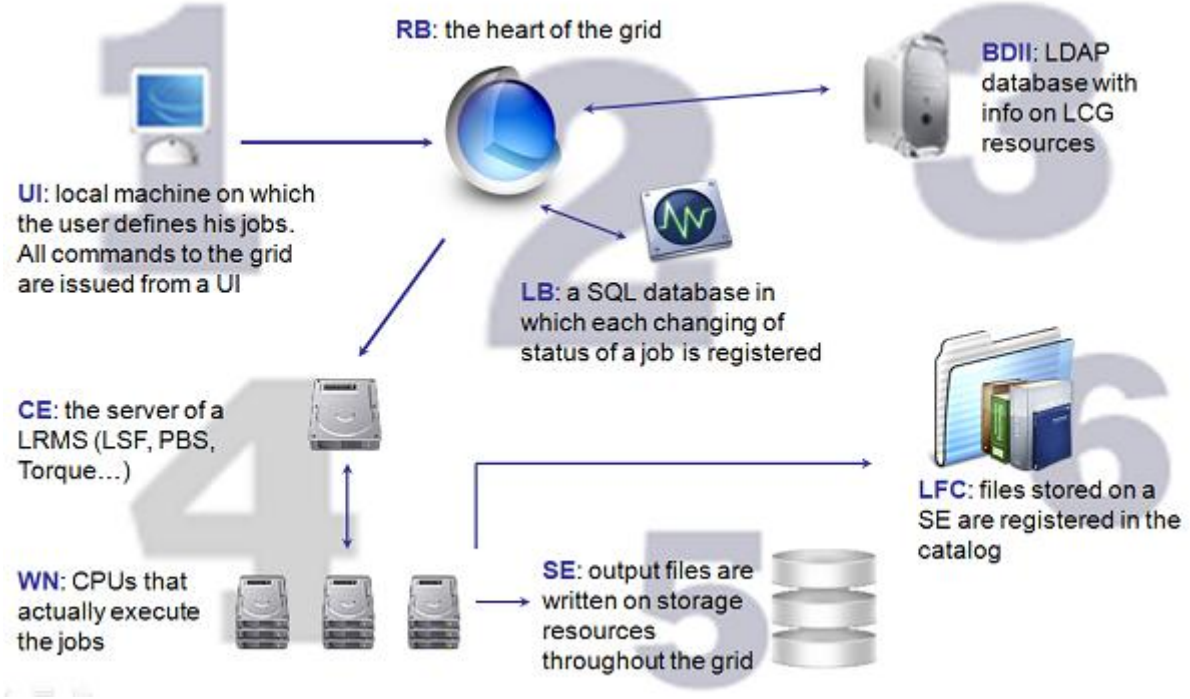

Figure 5.1: Picture of gLite workflow.

are registered in LCG file catalog (LFC), so that they will be avaiable to all grid users. One may then check if the job has really run as expected through the log files which are created and usually sent back to the RB and then to UI.

5.4 Distributed Data Management (DDM/DQ2)

The data on GRID must be well organized and just the storage elements serves to store it by an user or by an application for future retrieval. In gLite, every storage element must have a GSIFTP server, offering basically the same functionalitis of FTP but enhanced to support GSI security [2]. The structure of the data storing process is well-arranged. All the saved files are then registered in a catalog. A catalog is basically a database that maps the name of a file (LFN = logical file name) to its physical location (PFN = physical file name). Files in a catalog may have more than one LFN (in principle, it has nothing to do with its real name), they can have more than one replica. That is, the name of a file may be present on two different SE. What uniquely identifies them is the GUID (grid unique identifier, a string of 40 bytes). gLite supports two different types of catalogs which are not synchronized: LFC (LCG File Catalog) and RLS (Replica Location Server) in this description we will only deal with LFC, which is now the most used in ATLAS.The catalog can be accessed using data management commands from the UI. Two environment variables must be set: the file

- catalog type: $export\ LCG\_CATALOG\_TYPE = lfc$

[2]GSI = Globus Security Infrastructure

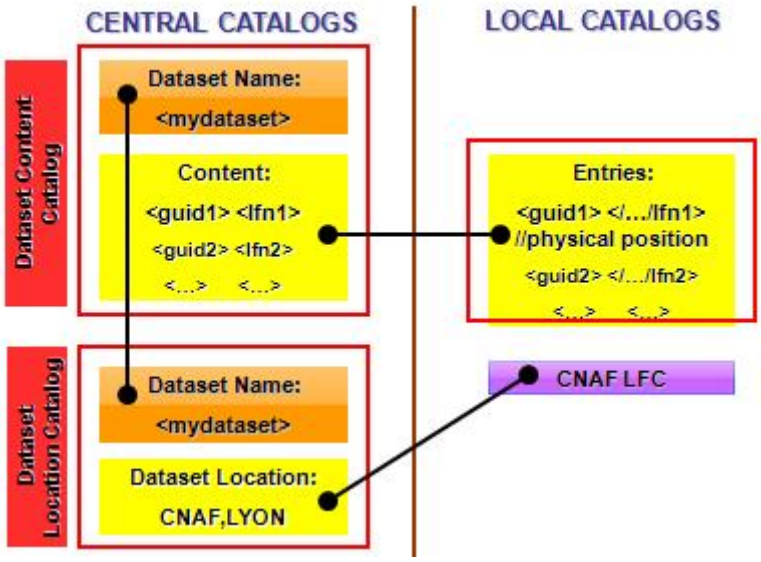

Figure 5.2: Connection between global dataset catalogs and local catalogs

- and its address: $export\ LFC\_HOST = lfc - atlas - test.cern.ch$

. LFN in LFC have a particular form: they are organized in hierarchical directory-like structure, having the following look $lfn : /grid/\langle VO\rangle / \langle dir\rangle / \langle filename\rangle$. The files in the LFC catalog can be due to this structure browsed as if they were in a unix filesystem $lfc-ls\ /grid/atlas$. When somebody wants two catalogs communicating one whit the other then must be set one more environment variable: $export\ LCG\_GFAL\_INFOSYS = \langle BDII\ \_address : 2170$.

ATLAS DDM moves from a file based system to one based on datasets. Dataset consist of more files and the DDM system provide then scalable global data discovery and access via a catalog hierarchy where is no global physical file replica catalog but global dataset replica catalog and global dataset location catalog. The structure is more deeply complicated but it id indeed useless to know all of this. It is enough to know the logical global hierarchy and names of 'dataset catalogs' and their functions see Figure 5.2. In LCG, the local replica catalog is the LCG File Catalog (LFC). Let us suppose a dataset A placed in site N but which is not present in site M, then when M subscribes to dataset A, it is transfered to this site and registered in catalogs.

DQ2 (DDM) stands a step higher than LFC. It is a database made up of different tables. Primary entities in DQ2 are the datasets, considered as bulks of similar files. The main table of DQ2 maps a dataset name (e.g., csc11.005001.pythia_minbias.simul.HITS.v11004202) to its "geographical" locations (CNAFDISK, CERNPROD, PICDISK,...). Then, another table contains, for each dataset, the list of its files and mapping between them and their guid in the local LFCs.

5.5 Production System

The production software is installed on roughly 80 of LCG sites. It allows members of ATLAS VO run the jobs and analysis on GRID. What is the job ? Job is any executable that will run on a grid resource. ATLAS production jobs can be of different types Mostly event generation, simulation + digitization done at the same step, reconstruction and finally analysis. Each part of the chain produces inputs for the subsequent one.

To specify arguments and requirements of some job we have to write the above mentioned JDL file. JDL file have to be written in a high-level language based on Class Advertisement (ClassAd) Language used to describe the jobs characteristics and constraints. The JDL file consists of lines of the form attribute = expression; The simplest possible JDL file for example called HelloWorld.jdl could looks like this one:

Executable = /bin/echo;
Arguments = Hello World!;
StdOutput = HelloWorld.out;
StdError = HelloWorld.err;
OutputSandbox = HelloWorld.out, HelloWorld.err;
VirtualOrganisation = atlas;

The job after its definition could be submiter on GRID by the command: $glite-wms-job-submit\ delegationid\ \langle delegateID\rangle\ HelloWorld.jdl$. When it is submitted the RB returns a job unique identifies JobID which takes the form $https://\langle RB\_name\rangle:9000/\langle unique\_string\rangle$ In the time the job runs we are able to check the status of the job and investigate more about its place of run etc. by using gLite tools (commands). [3].

Now I would like to introduced the architecture of the production system see Figure 5.3. Through the Oracle SQL queries they could be managed by Eowyn, which is the brain of the production system. Eowyn submit the jobs under GRID, pick up free jobs from the database, validate finished jobs and ask executor about the status of the job. Then there are 3 kind of plugins for Eowyn = executors provides the supervisor production system (Dulcinea, Panda and Lexor-CondorG). Executors tell Eowyn how many jobs can be submitted on the corresponding grid and submit them.

The jobs are grouped in ”datasets” and ”tasks” (= dataset) which are reprezentatives of the jobs of the same kind. In order to collect informations on tasks and jobs supervisor uses 3 tables: ETASK = list of the task, EJOBDEF = list of the job for all the datasets to be produced and as link to entry dataset to job table and to have the task uniquely identified is used TASKID number, and finally the table TASKFK which contains all the job related to the dataset to be execute. In the table are much more fields which are important in case of one would like monitoring and investigating task problems (this is done by so-called shifters).

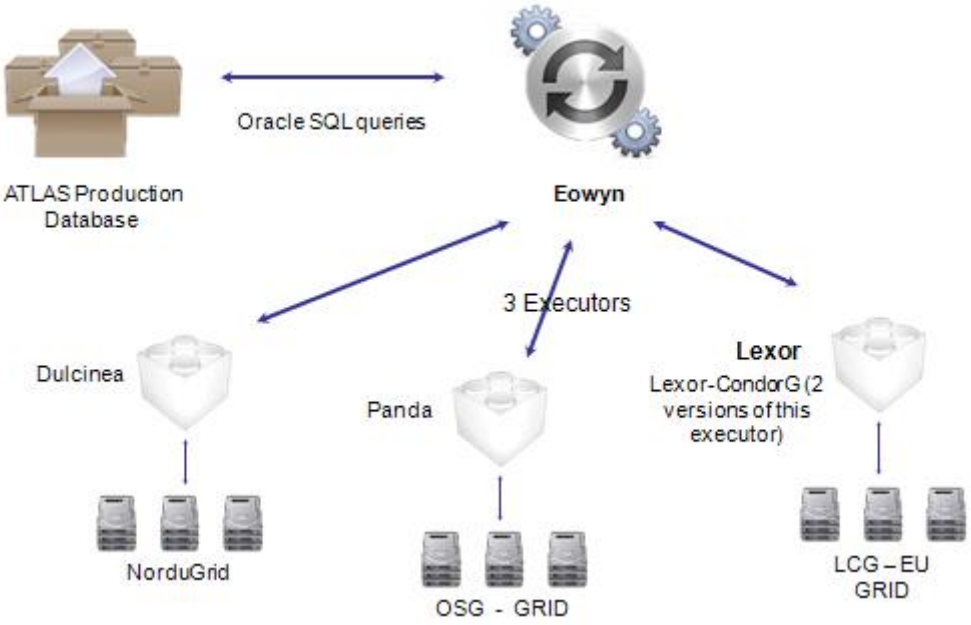

Figure 5.3: The architecture of the Production system.

5.5.1 Brief look at Workload and Data management shift

Workload management system is the servise that matches resources with jobs using RB, keeps track of the status of jobs (LB service), talks to the batch systems on the remote sites (CE), matches jobs with sites where data and resources are available and if jobs fail then the WM service re-submits it. For want of storing huge amount of data distributed in many sites Data management system presents the solution consisting of the SE resources which have to provide a good access and services to storage spaces and of the middleware which has to be able to manage different storage systems uniformly and transparently for the user. The dissimilarity of the infrastructure of the sites causes the different storage system implementation. Usually the biggest and complex storage systems are owned by T1 sites as is Mass Storage System (MSS) as CASTOR or DCACHE. For T2 centers disk arrays such as Disk Pool Managers (DPM) have been developed. To hide the different implementations all the SEs are managed by the Storage Resource Manager (SRM) ensuring the space reservation and file pinning.

Jobs can fail for many different causes. People running production are asked to check the failure reasons and try to fix them and it if the duty of so-called 'shifter'. Problems can occur in different part of the system: there may be bugs in the Athena software, inefficiencies in some grid service, system commands hanging up . . . etc. Each of these inconveniences is treated in a different way.

To understand the kind of problem that a failed job found some informations can be found

[3] glite-wms-job-... = lcg-wms-job-... presently only two conventions

in the Production database, checking the fields in the EJOBEXE table. These two informations may be enough to understand the failure reasons. But what went wrong if the error fields in this table is not enough to understand the reason ? For this case every job has 2 different log files: GridWrapper.log and jobName.log. The former is the log of the grid job, so it contains all the informations of the setup of the environment on the WN, of the launching of the Atlas software and of the registration of the output files. It is retrieved by Lexor on our UI. The latter is the log of the Athena executable. Powerful scripts help then an operator to manage failed jobs.

Actually, OSG does not use a proper executor, they use Eowyn for picking up the jobs from the production database, then Eowyn passes the jobs to Panda, which is a complete framework that can do almost everything, from submitting the jobs to doing analysis. Panda has a plugin that makes the communication with Eowyn possible. LCG and NorduGrid, instead, use just an executor Lexor and Dulcinea, which are much like plugins that interface Eowyn with the underlying grid. On LCG and NG the analysis is done using Ganga. Presently, beside Lexor, there are other 2 executors on LCG, both based on Condor (they do not use the WMS, the ”brain” of LCG). They are Lexor-CondorG and Cronus. A discussion is going on on which of the three to use (Lexor, Lexor-CG and Cronus). For more information about the 'DDM Shift instructions' is possible to see paper with useful 'manual' and description created by me and my colleague [50].

5.6 Ganga

Ganga (*G*audi/*A*thena and *G*rid *A*lliance) is an interface to the grid that is being developed jointly by ATLAS and LHCb [44]. This interface is powerful tool for manage jobs that use the Gaudi/Athena Framework on grid. This python utility help configuring, submitting analysis jobs and provide access to all the information about the track of what user have done without all technicalities. Moreover there are many plugins for Atlas and LHCb and tools for example for easier job building, pre-defined configurations and in particular single desktop for a variety of tasks with friendly interface. This interface does not depend on the user's preferences. One have the possibility to work in an enhanced Python shell, with scripts which is very good to see how the system really works or even through a Graphical User Interface (GUI). A job in Ganga is constructed from a set of building blocks, not all required for every job they are illustrated in the picture 5.5. Ganga provides a framework for handling different types of Application, Backend, Dataset, Splitter and Merger, implemented as plugin classes. Running of a particular Application on a given Backend is enabled by implementing an appropriate adapter component or Runtime Handler see Figure 5.5. The JobOptions file could be simly modified in order to connect Ganga with Atlantis. Then when the job is successfully completed Ganga could retrieve the JiveXML files to the job's output directory. They after unzipping produce a single file which Atlantis will then be able to use as its input.

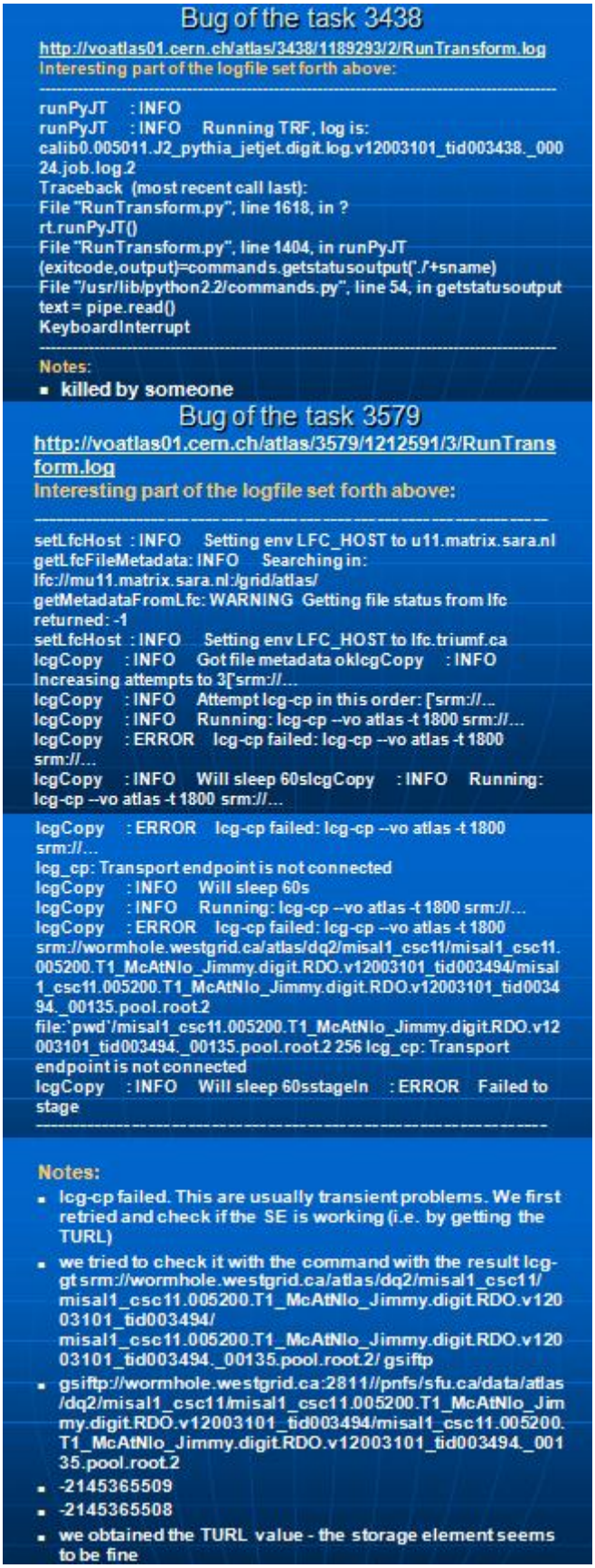

Figure 5.4: Simple picture of bugs of tasks taken over presentation created by me on combined WM/DDM GRID shift.

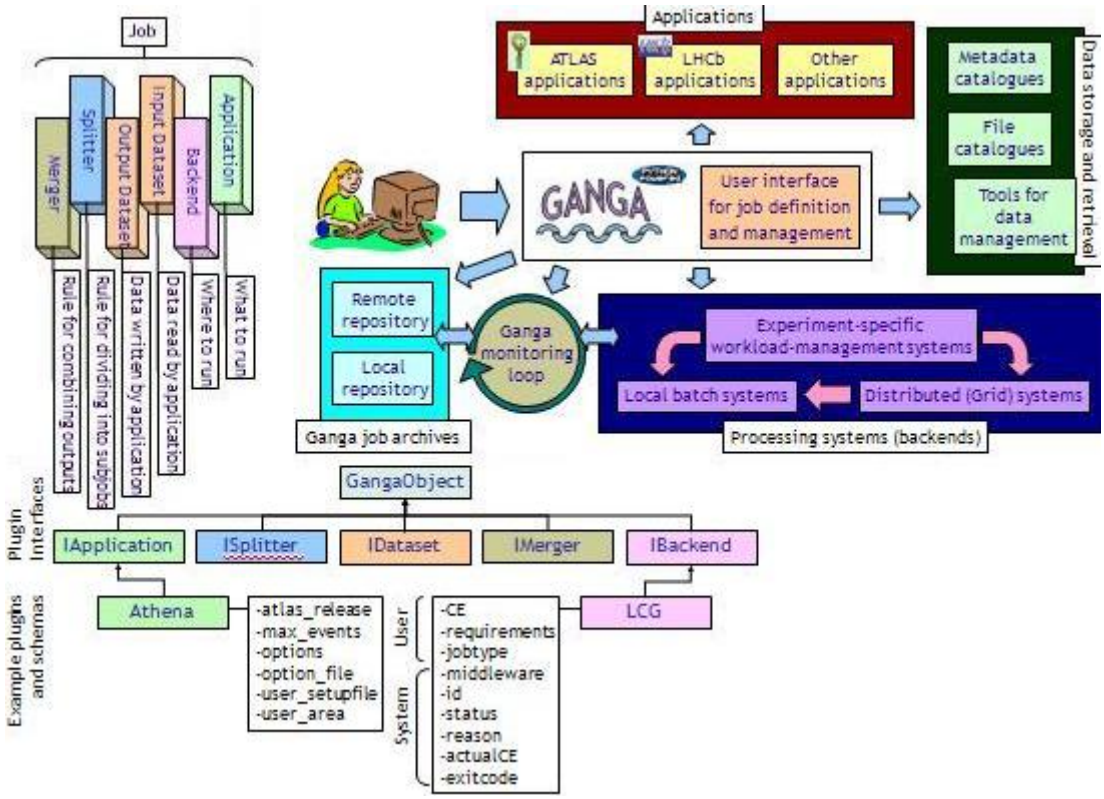

Figure 5.5: Ganga implemented into the whole computing architecture, its customisation flexibility and the design of a job is shown here.

Chapter 6

Thesis Summary

In the first chapter of this thesis I tried to introduce the theory of the Standard Model as simple as possible. I try to provide something like a simple framework of the theory in order to catch the basic cogitations of the greatest scientific achievements of the twentieth century. My intention was go through the theory keeping the idea of symetry in the nature. The predictions of the SM was very well verified by many experiments as LEP, BaBar, Tevatron etc. But as mentioned there are still many unanswered questions to investigate. Does the Higgs boson exist ? This particle plays important role in the mechanism of the spontaneous symmetry breaking. What about the new physics behind the SM ? The CP violation puts with its existence a unified and unbiased attack on new physics at the top of the triengle. This existence may be tested through the possible discoveries like neutrino mass mixing and more flavour mixing phases etc.

From the theory describing the CP violation I move to the experiment in the second chapter. One of the main motivations for the CP violation experiments was the revelation of the CPV mechanism by B decays. Since there exist $B^0\overline{B}^0$ mixing is it one of the very powerful ways to explore the CP violation through B-decays. Since one of my interest is the practical modern physics and their tools I decided to analyze one up to now well measured decay of B^+ meson.

Third chapter is focused on the largest experimental equipment that have been ever built and start its operation during the year 2008. I described there more deeply all the important components of these experiments. And one of my unfortunately not so evident effort was to connect the description with the function of the described part of the equipment.

Next chapter is dedicated to the ATLAS computing system. I only sketch here the data acquisition system with the brief information about triggers. Before I came to the GRID computing I put here only a few comments to the ATLAS analysis model which says in general where to start with the analysis and refers to a very useful tools.

The last chapter is devoted to one of the important constituents of the all experimental equipments - GRID. It is really very important to develop such a powerful tool. Otherwise we would not be able to store the enormous data from the LHC experiments and analyze them. With huge amount of estimated production of LHC run, really only the GRID allows us precise study of the outcome of the proton-proton collisions, which is the target of the LHC project. I defined here all of the unavoidable basic steps to follow for develop system like GRID. Since I participated in shifts, I tried to implement here some of the live production and embraced the whole

chapter as summary of the really basics with some 'how to' upgrade. At the end is given an information on Ganga tool.

Bibliography

[1] J. Blank, P. Exner, M. Havlíček, *Hilbert-Space Operators in Quantum Physics*, American Institute of Physics, 1994

[2] J. Chýla, *Quarks, partons and Quantum Chromodynamics*, lecture notes, http://www-hep2.fzu.cz/Theory/notes/text.pdf

[3] S. F. Novaes, *Standard model: An introduction*, 10th Jorge Andre Swieca Summer School: Particle and Fields, Sao Paulo, Brazil, 31/1 - 12/2 1999, hep-ph/0001283

[4] Mikio NAKAHARA *GEOMETRY, TOPOLOGY AND PHYSICS, Second Edition*, Department of Physics Kinki University, Osaka, Japan, 2002.

[5] B.R.Martin& G.Shaw *Particle Physics, SECOND EDITION*, Department of Physics and Astronomy, University College London, Department of Theoretical Physics, University of Manchester, reprinted March 2003.

[6] Guy D.Coughlan, James E.Dodd, Ben M.Gripaios *The Ideas of Particle Physics An Introduction for Scientists, Third edition*, Cambridge University Press, 2006.

[7] Yuval NE'EMAN and Yoram Kirsh *The Particle Hunters, Second edition*, Cambridge University Press, 1996.

[8] W-M Yao *et al* 2006 *J. Phys G: Nucl. Part. Phys.* 33 1 http://stacks.iop.org/JPhysG33/1

[9] *Determination of the* $B_d^0 \rightarrow D^* l\nu$ *Decay Width and* $|V_{cb}|$,arXiv:hep-ex/0210040 v1 16 Oct 2002

[10] *A measurement of the* $B^0\overline{B}^0$ *oscillation frequency and determination of flavor-tagging efficiency using semileptonic and hadronic* B^0 *decays* ,BABAR-CONF-00/08, SLAC-PUB-8530, August 8, 2000

[11] *Measurement of the* $B_d^0 - \overline{B}_d^0$ *Oscillation Frequency* ,CERN-EP/98-28 (revised), March 23, 1998

[12] *Writing B-physics analysis code in Athena* ,CERN-EP/98-28 (revised), March 23, 1998

[13] http://documents.cern.ch/cgi-bin/

[14] S. Eidelman *et al.*, Physics Letters B592, 1 (2004)

[15] *Rare B Decays into States Containing a* J/ψ *Meson and a Meson with* $s\overline{s}$ *Quark Content*, BABAR-PUB-02/07, SLAC-PUB-9262, hep-ex/0000000

[16] *Exclusive Semileptonic and Rare B-Meson Decays in QCD*, arXiv:hep-ph/9805422 v2 10 Jul 1998

[17] *Standard model matrix elements for neutral B-meson mixing and associated decay constants*, arXiv:hep-ph/0011086 v2 28 Feb 2002

[18] *CP Violation and B Physics at the LHC*,arXiv:hep-ph/0703112v1 12 Mar 2007

[19] *Flavour Dynamics: CP Violation and Rare Decays*, arXiv:hep-ph/0101336 v1 30 Jan 2001

[20] *RARE B DECAYS AT BELLE*, arXiv:hep-ex/0205033 v3 21 May 2002

[21] J/ψ *Production at LEP: Revisited and Resummed*, arXiv:hep-ph/9810364 v2 19 Oct 1998

[22] http://atlas-computing.web.cern.ch/atlas-computing/projects/twikiUtils/

[23] https://twiki.cern.ch/

[24] http://castor.web.cern.ch/castor/DOCUMENTATION/

[25] http://pdg.lbl.gov/

[26] http://glite.web.cern.ch/glite/

[27] https://gus.fzk.de/pages/home.php

[28] http://grid-deployment.web.cern.ch/grid-deployment/documentation/

[29] http://lcg.web.cern.ch/LCG/

[30] http://gridui02.usatlas.bnl.gov:25880/server/pandamon/

[31] http://dashb-atlas-data.cern.ch/dashboard/request.py/site

[32] http://www.slac.stanford.edu/xorg/hfag/rare/index.html

[33] http://atlas.ch/

[34] http://aliceinfo.cern.ch/

[35] http://cms.cern.ch/

[36] http://lhcb.web.cern.ch/lhcb/

[37] http://agenda.cern.ch/tools/SSLPdisplay.php?stdate=2006-07-03&nbweeks=6

[38] https://twiki.cern.ch/twiki/bin/view/Atlas/TriggerDAQ

[39] http://www.hep.ucl.ac.uk/atlas/atlantis/

[40] http://www.thep.lu.se/ torbjorn/Pythia.html

[41] http://atlas-computing.web.cern.ch/atlas-computing//documentation/swDoc/

[42] http://root.cern.ch/

[43] http://proj-gaudi.web.cern.ch/proj-gaudi/

[44] https://twiki.cern.ch/twiki/bin/view/Atlas/DistributedAnalysisUsingGanga

[45] http://projects-docdb.fnal.gov/cgi-bin/ShowDocument?docid=91

[46] https://twiki.cern.ch/twiki/bin/view/Atlas/GangaWithAtlantis

[47] http://ganga.web.cern.ch/ganga/presentations/index.html

[48] http://ganga.web.cern.ch/ganga/documents/index.html

[49] http://en.wikipedia.org/wiki/Main_Page

[50] https://twiki.cern.ch/twiki/pub/Atlas/AtlasComputingOperationsCZ/
DDM_Shift_Instructions.pdf